nature communications

Article

https://doi.org/10.1038/s41467-026-69316-0

Preoptic kisspeptin-nNOS-GnRH (KiNG) neuronal network regulates LH rhythmicity through activation-inhibition in mice

Received: 22 February 2024

Accepted: 29 January 2026

Published online: 10 February 2026

Check for updates

Virginia Delli[1], Marie Moulinier[2], Anna-Maria Lazaridou[1], Charles-Antoine Seux[1], Sooraj Nair[1], Tori Lhomme[1], Julien Dehame[1], Daniela Fernandois[1], S. Rasika[1], Damien Lemoine[1], Alan Carleton[2] & Konstantina Chachlaki[1]

Gonadotropin-releasing hormone (GnRH) neurons are the final target of a complex network regulating reproduction. The balance between excitatory and inhibitory inputs is essential for rhythmic GnRH secretion, including pulses and surges, yet the underlying mechanisms remain unresolved. Here, using adult animals of both sexes, we test the hypothesis that excitatory kisspeptin and inhibitory neuronal nitric oxide (NO) synthase (nNOS)-derived inputs orchestrate GnRH release within a microcircuit of kisspeptin, nNOS and GnRH neurons (the "KiNG" network). We focus on nNOS neurons of the organum vasculosum of the lamina terminalis (OV) and the median preoptic nucleus (MePO), which interact with kisspeptin and exhibit cycle-dependent kisspeptin receptor (Kiss1r) expression. Using a highly-sensitive NO/cGMP biosensor together with electrophysiological, genetic, chemogenetic and pharmacological approaches we demonstrate that kisspeptin induces NO-dependent cGMP production in the OV/MePO, including in GnRH neurons, which in turn fine-tunes the GnRH/LH response, providing mechanistic insights into how the KiNG network shapes pulse and surge generation.

Gonadotropin-releasing hormone (GnRH) neurons of the hypothalamus orchestrate reproduction. While their cell bodies are mainly distributed in the preoptic region, their nerve terminals, which lie in the median eminence of the hypothalamus, release the GnRH decapeptide in a rhythmic manner into the pituitary portal capillary system[1,2]. Blood-borne GnRH acts on gonadotrophs in the anterior pituitary, stimulating the synthesis and secretion of the gonadotropins, luteinizing hormone (LH) and follicle-stimulating hormone (FSH). The release pattern of GnRH includes both pulse and surge phases in females but only pulses in males. This GnRH rhythmicity arises from the integration of a complex array of excitatory and inhibitory inputs from both the central nervous system (e.g., kisspeptin and nitric oxide [NO]) and peripheral organs (e.g., estrogen and testosterone from the gonads). The correct balance of these signals is indispensable for the timely and appropriate release of LH and FSH, which are key to the establishment and proper function of the hypothalamic-pituitary-gonadal (HPG) axis.

The stimulatory effect of kisspeptin-kisspeptin receptor (Kiss1-Kiss1r) signaling on GnRH activity and secretion is fundamental to inducing LH release[3], crucial for the establishment and maintenance of reproduction[4–6]. However, this function requires GnRH/LH pulses rather than prolonged and sustained kisspeptin-induced GnRH activation, which shuts down the axis, suggesting the existence of an "OFF" switch. It is known that kisspeptin neurons of the anteroventral periventricular nucleus (AVPV) are important components of the mechanism mediating the positive feedback effects of estrogen on the preovulatory GnRH/LH surge, while the subpopulation of kisspeptin neurons in the arcuate nucleus (ARH), frequently referred to as KNDy neurons due to their coexpression of kisspeptin, neurokinin B and dynorphin, has been associated with the control of pulsatile LH

[1]Univ.Lille, CHU Lille, Inserm, Laboratory of Development and Plasticity of the Neuroendocrine Brain, Lille Neuroscience and Cognition, UMR-S 1172, Lille, France. [2]Department of Basic Neurosciences, Faculty of Medicine, University of Geneva, Geneva, Switzerland. e-mail: Konstantina.Chachlaki@inserm.fr

secretion during the negative feedback phase of estrogen[7,8]. While the activatory role of kisspeptin is well established, the negative regulators of the GnRH system that terminate the kisspeptin response remain largely understudied. For example, the KNDy neuronal hypothesis can explain the control of kisspeptin neurons themselves but not how GnRH neurons are controlled[9], since dynorphin is not necessary for the termination of the GnRH/LH pulses in rodents[10] and in addition, is lacking in human KNDy neurons[11]. There is, therefore, a knowledge gap regarding the intricate regulatory network governing GnRH neuronal activity and hence the mechanisms that shape the GnRH surge and pulse.

In a recent review, we postulated the existence of a Kisspeptin-nNOS-GnRH or "KiNG" neuronal network that would function by alternating between neuronal activation and tonic inhibition in order to modulate LH pulse and surge generation[12]. Similar to kisspeptin, neurons expressing the neuronal NO synthase (nNOS, coded by *Nos1*), which produce the highly diffusible gaseous messenger NO, are estradiol-sensitive and express the estrogen receptor alpha (ERα)[13]. nNOS neurons are morphologically and functionally associated with GnRH neuronal cell bodies and dendrites in the median preoptic nucleus (MePO) and the organum vasculosum of the lamina terminalis (OV); NO acts as an inhibitory signal that rapidly integrates and transmits peripheral signals to the brain, particularly to GnRH neurons[14]. Once produced, NO diffuses to neighboring cells where it binds and activates soluble guanylate cyclase (sGC), leading to the generation of the second messenger cyclic guanosine monophosphate (cGMP). The amplitude and duration of this NO/cGMP signal are further shaped by phosphodiesterases (PDEs) such as PDE5, which degrade cGMP and thereby terminate the response[15]. Because GnRH neurons are widely dispersed across the preoptic area a diffusible messenger like NO is well positioned to coordinate their activity. The importance of NO signaling in the regulation of GnRH functionality is increasingly apparent (for review see ref. 14) and loss-of-function mutations in *Nos1* have recently been identified in a cohort of patients with congenital hypogonadotropic hypogonadism[16], demonstrating the key role of nNOS in reproduction. This hypogonadotropic hypogonadal phenotype also occurs in mice genetically deficient for Nos1 (*Nos1*$^{-/-}$)[16–18], which exhibit both abnormal estrous cyclicity and blunted LH levels in proestrus[16] while the intracerebroventricular injection of NOS blockers inhibits GnRH/LH secretion[19], suggesting that nNOS activity and NO release are involved in both the positive and negative feedback effects of estrogen. In fact, estradiol positively regulates nNOS activity in the OV/MePO by promoting the physical association of the nNOS enzyme with the NMDA receptor[20,21] and subsequently, the phosphorylation of nNOS at Ser-1412[22], an action that requires Kiss1-Kiss1r signaling[17]. Kisspeptin-NO interactions have also been identified as a mechanism shaping GnRH pulsatility by modulating the refractory period of GnRH neuronal activity in response to kisspeptinergic stimuli[23], supporting the so-called KiNG neuronal network hypothesis, i.e., the possibility that a microcircuit of excitatory and inhibitory inputs from kisspeptin and nNOS neurons could orchestrate GnRH neuronal activity and release[12].

In this report, we test this hypothesis by focusing on the preoptic OV/MePO nNOS population (nNOS$^{OV/MePO}$), surrounding the GnRH cell bodies. Using in situ hybridization and various in vivo genetic and chemogenetic approaches, we examine the role of the nNOS$^{OV/MePO}$ neurons in the control of pulsatile and kisspeptin-induced LH secretion, and uncover mechanistic details of the KiNG neuronal network, thanks to a viral tool engineered to measure in vivo NO/cGMP release.

Results

Cycle-dependent Kiss1r expression in preoptic Nos1-expressing neurons

nNOS enzymatic activity in the OV/MePO, and hence NO levels, have been suggested to be controlled by the classic Kiss1/Kiss1r/AKT pathway[17], being low during diestrus I (Di) and reaching their maximum during proestrus (Pro)[22]. In order to more accurately analyze the anatomical relationship between neurons expressing *Kiss1*, *Kiss1r*, and *Nos1* mRNA in the hypothalamic preoptic area and evaluate plausible differential dynamics across the estrous cycle, we took advantage of RNAscope technology. Fluorescence in situ hybridization in the OV and MePO of cycling females revealed the expression of *Kiss1r* mRNA in a fair proportion of *Nos1*-positive cells (Fig. 1A, B, Suppl. Fig. 2A). Interestingly, even though the percentage of *Nos1*- or *Kiss1r*-expressing cells remained unaltered across the estrous cycle (Fig. 1C, D), the percentage of *Nos1*- expressing cells also positive for *Kiss1r* mRNA was significantly increased in proestrus, while no marked difference was seen between the metestrus (mE) and diestrus stages (OV: 44.0 ± 2.5 % in mE, 45.1 ± 1.3 % in Di vs. 55.2 ± 1.1 % in Pro, $p = 0.02$ and $p = 0.01$, respectively; MePO: 45.4 ± 1.6 % in mE, 44.9 ± 4.5 % in Di vs. 58.8 ± 3.4 % in Pro, $p = 0.02$ and $p = 0.06$, respectively) (Fig. 1B). Similar to metestrous and diestrous females, male mice demonstrated lower levels of co-expression between the *Nos1* and *Kiss1r* mRNAs (OV: 36.5 ± 2.5 % and MePO: 30.0 ± 3.1 %) (Fig. 1B).

These changes were specific for the nNOS population of the OV/MePO (nNOS$^{OV/MePO}$). In the hypothalamic AVPV, the percentage of *Nos1*-expressing cells co-expressing *Kiss1r* mRNA was found to be unaltered between diestrus and proestrus (41.9 ± 1.8 % in Di vs. 44.5 ± 2.2 % in Pro) (Suppl. Figs. 1A, C–E and 2B). Even though *Kiss1* and *Nos1* mRNAs were found to be separately expressed in the vast majority of cells in the AVPV (Suppl. Fig. 1B, E–G), <10 % of *Kiss1*-positive cells were seen to express low amounts of *Nos1* mRNA at both stages of the estrous cycle (7.8 ± 2.1 % in Di, vs. 6.1 ± 1.6 % in Pro, $p = 0.5$), with *Kiss1* mRNA showing an almost 50% increase in proestrus (13.2 ± 1.8 % in Di, vs. 21.3 ± 1.8 % in Pro, $p = 0.03$) (Suppl. Fig. 1F).

Kisspeptin drives NO-dependent cGMP production in OV/MePO neurons

Previous reports have revealed that the intraperitoneal administration of the decapeptide form of kisspeptin (kisspeptin-10, kp-10) promotes an increase in nNOS phosphorylation at Ser1412 in the OV/MePO, accompanied by an increase in LH levels[17], an effect that we also observe in our model (Fig. 1E–H) in keeping with the frequent coexpression of *Kiss1r* in these neurons (Fig. 1). Phosphorylation at Ser1412 is believed to be associated with enhanced nNOS enzymatic activity[24]. However, the association of Ser1412-phosphorylation of nNOS with hypothalamic NO production has not been demonstrated in vivo. We therefore engineered an AAV9 viral tool expressing the cGMP-dependent biosensor, FlincG3 (Fig. 2A), which we have previously used to accurately measure levels of NO released by transfected cells in vitro[16,25], under the control of the CMV promoter. Stereotaxic injection of the virus expressing the FlincG3 construct into the OV/MePO of adult male mice allowed us to perform ex-vivo cGMP imaging on living brain slices (Fig. 2B, C). Live imaging revealed the presence of basal levels of FlincG3 fluorescence in the OV (Fig. 2D). Bath application of a high concentration of the NO donor PAPA/NO (5 µM) resulted in an increase in fluorescence as a consequence of local NO-stimulated cGMP production (Fig. 2D, E). This increase was prevented when PAPA/NO was applied together with the sGC inhibitor ODQ (10 µM), confirming that the FlincG3 fluorescence was a result of NO/cGMP production (Fig. 2D, E). We then took advantage of this technology to verify whether kisspeptin-induced nNOS activation actually results in NO/cGMP release. Bath application of kp-10 (10 nM) resulted in a > 200% increase in the maximum FlincG3 ΔF/F0 (change in fluorescence relative to baseline) values in the OV (mean baseline ΔF/F0 = 0.006 ± 0.002 vs. mean kp-10 ΔF/F0 = 0.03 ± 0.002) (Fig. 2F). Bath application of ODQ before kp-10 administration completely blocked the kp-10-induced increase in FlincG3 fluorescence (Fig. 2G).

https://doi.org/10.1038/s41467-026-69316-0

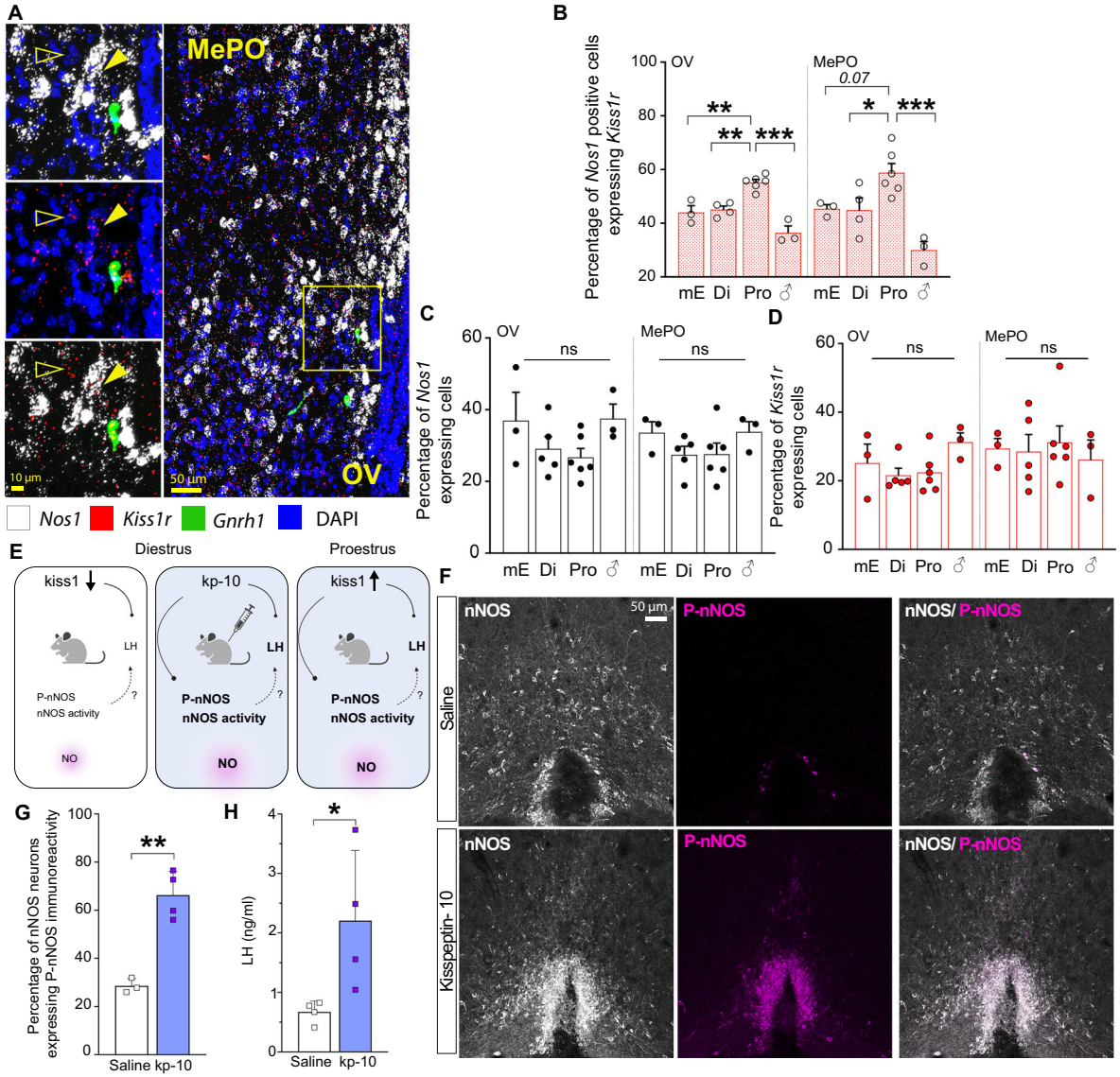

Fig. 1 | Kisspeptin-nNOS interaction dynamics in the preoptic area of the cycling female mouse. A–D Anatomical interaction and differential expression of *Nos1*, *Kiss1* and *Kiss1r* mRNAs in the female mouse preoptic area across the estrous cycle. **A** Confocal fluorescent RNAscope reveals the expression of *Kiss1r* mRNA expression in cells co-expressing variable amounts of *Nos1* mRNA in the OV/MePO during diestrus. Nuclei are counterstained with DAPI. Magnifications on the right side of the illustrations indicate representative examples of *Nos1* mRNA positive cells co-expressing the *Kiss1r* mRNA (solid arrowheads), also co-expressed by *Gnrh1*- positive neurons as well as *Nos1*- negative cells (open arrowheads). **B** Quantification of the percentage of cells positive for *Nos1* mRNA also positive for *Kiss1r* mRNA in metestrus, diestrus and proestrus in female, and in male mice in the OV and MePO (One-way ANOVA, Dunnett's multiple comparisons test, respectively: $F_{(3, 12)} = 23.79$ $p < 0.001$, $F_{(3, 12)} = 10.32$; $p = 0.001$; post hoc test: mE vs. Pro: $p = 0.001$ and $p = 0.07$ $n = 3, 6$; Di vs Pro: $p = 0.001$ and $p = 0.04$ $n = 4, 6$; males vs Pro: $p < 0.001$ and $p < 0.001$ $n = 3, 6$). **C**, **D** Quantification of the percentage of DAPI-stained cells positive for (**C**) *Nos1* and (**D**) *Kiss1r* mRNAs in metestrus ($n = 3$), diestrus ($n = 5$) and proestrus ($n = 6$) in female and male ($n = 3$) mice in the OV and MePO (One-way ANOVA, Dunnett's multiple comparisons test). **E–H** Kisspeptin effect on nNOS activity in the mouse preoptic area. **E** Graphic illustrating the proposed mechanism of action of physiological kisspeptin fluctuations during diestrus or proestrus, or of peripheral kp-10 (1 nmol) administration on nNOS activity. **F** Immunolabeling for nNOS and P-nNOS in the OV/MePO of female mice upon intraperitoneal administration of saline or kp-10 (**G**) Quantification of the ratio of P-nNOS immunoreactive cells to the total number of nNOS cells (two-tailed unpaired t-test $t_{(5)} = 6.26$ $p = 0.002$; $n = 3, 4$) and (**H**) circulating LH levels in mice 30 min after a peripheral injection of kp-10 (two-tailed unpaired t-test, $t_{(6)} = 2.57$, $p = 0.04$, $n = 4, 4$). Values indicate means ± SEM. ns: non-significant, $p > 0.05$, $^{*}p < 0.05$, $^{**}p < 0.01$. Source data are provided as a Source Data file. Schematic illustrations created in BioRender. *Chachlaki, K. (2026)* https://BioRender.com/*arnv9ca*. OV, organum vasculosum laminae terminalis. MePO, median preoptic nucleus. kp-10, kisspeptin-10. NO, nitric oxide. P-nNOS, phosphorylated nNOS. Metestrus, mE. Diestrus, Di. Proestrus, Pro.

In order to determine whether cGMP is synthesized in cells different from those expressing the nNOS protein, and thus whether NO acts in a paracrine manner to stimulate the synthesis of cGMP, we analyzed the anatomical distribution of cGMP-producing cells in the OV/MePO of cycling females after local stereotaxic injections of the FlincG3 construct (Fig. 2H). Females were perfused during diestrus, when nNOS enzymatic activity and NO release are at their nadir, after a bolus intraperitoneal injection of saline or kp-10 (1 nmol; Fig. 2H). Kp-10 administration led to an increase in Ser1412-phosphorylation of the nNOS protein in the OV/MePO, as well as circulating LH levels, in agreement with previous reports (Fig. 1E–H)[17]. In accordance with our live imaging data, kisspeptin treatment was also accompanied by massive cGMP production in the OV/MePO (Fig. 2I–L) as attested to by the 250% increase in FlincG3 integrated fluorescence intensity (IntDens saline = 47.6 ± 13.8 vs. kp-10 = 168.8 ± 28.7) (Fig. 2J). Interestingly, FlincG3 fluorescence was rarely seen in nNOS-immunoreactive cells

https://doi.org/10.1038/s41467-026-69316-0

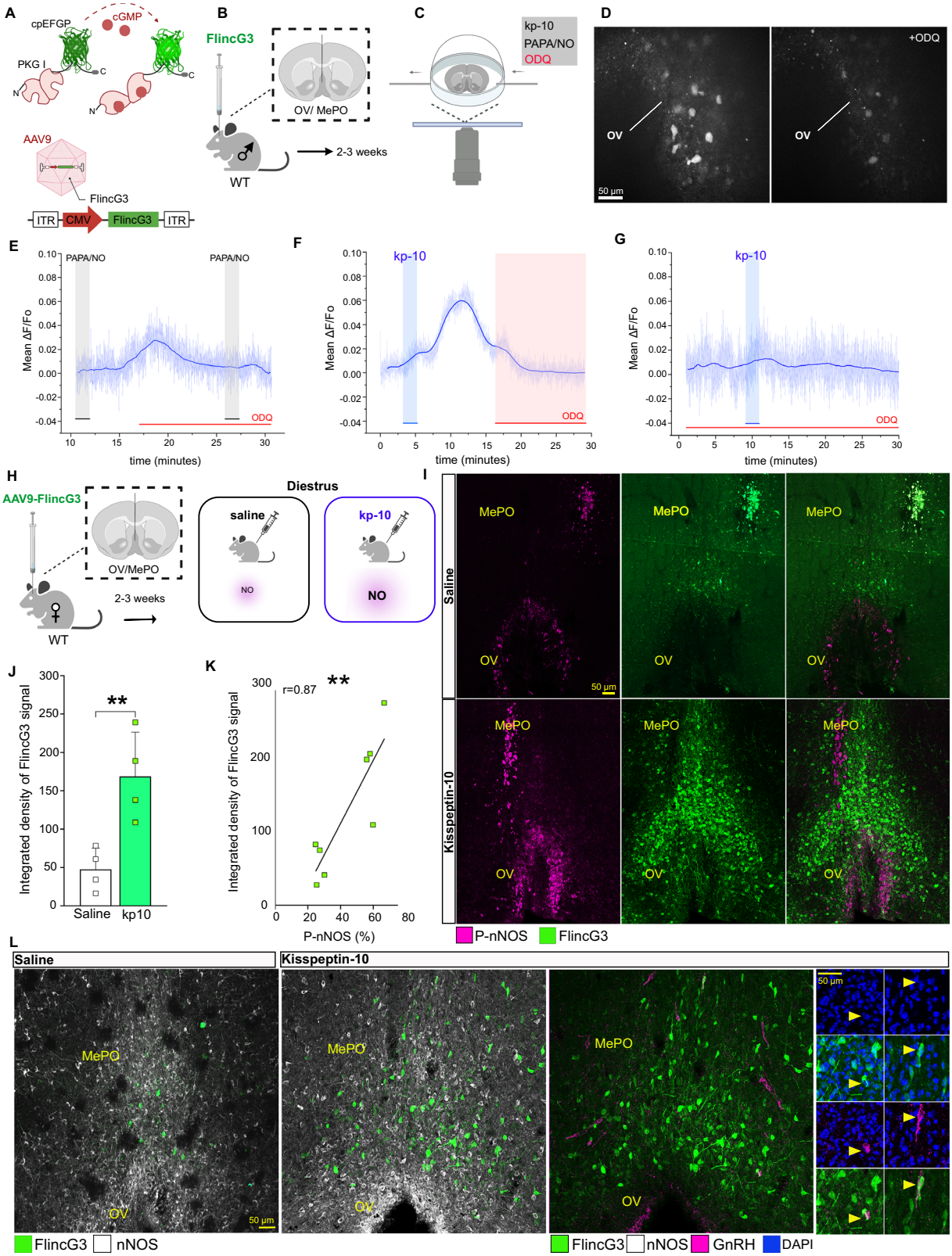

(OV: 1.6 ± 0.5 % and MePO: 4.0 ± 0.7 % of nNOS neurons showing FlincG3 signal) but was instead observed in cells surrounding nNOS-expressing neurons, including, strikingly, GnRH neurons (14.4 ± 3.2 % of GnRH neurons showing FlincG3 signal) (Fig. 2L). Notably, the-FlincG3 intensity was positively correlated with the levels of phosphorylation of the nNOS enzyme following kp-10 administration (Fig. 2I, K). Our observations demonstrate that cGMP production is coupled with the phosphorylation of nNOS protein at Ser1412 in vivo, and further support the hypothesis that kisspeptin, by modulating nNOS enzymatic activity, can directly increase local NO/cGMP levels. Altogether, these results provide further support for the existence of a kisspeptin-NO-GnRH communication network in the OV/MePO, as postulated in the KiNG hypothesis.

Fig. 2 | Kisspeptin-10 promotes nNOS activation and the subsequent production of cGMP. A Illustration of the molecular functioning of the FlincG3 protein and the construction of the viral vector driving its expression. **B** Graphical illustration of ex vivo live imaging in brain slices from WT male mice having received an intracerebral injection of AAV9-FlincG3 into the OV/MePO, and **C** schematic showing the brain slice (200-µm-thick) containing the OV/MePO in the perfusion chamber. **D** Fluorescent image of the brain slice containing cells expressing the FlincG3 protein, imaged in the absence or presence of ODQ (10 µM). **E**–**G** Data plots show ΔF/F0 in responder cells ($n = 3$ mice, $n = 5$–7 cells) upon application of kp-10 (10 nM) or PAPA/NO (5 µM) in the absence and presence of ODQ (10 µM). Experiment was independently repeated three times with similar results. **H** Graphical illustration of in situ imaging in WT females in diestrus, having received an intracerebral injection of AAV9-FlincG3 into the OV/MePO and sacrificed after peripheral administration of saline or kp-10 (1 nmol). **J** Quantification of the integrated intensity of the endogenous fluorescence of the FlincG3 protein in the OV/MePO, upon application of saline or kp-10 (two-tailed unpaired t-test $t_{(6)} = 3.80$ $p = 0.009$; $n = 4$) and (**K**) Correlation of the percentage of nNOS phosphorylation with the integrated density of the FlincG3 signal upon application of kp-10 (Pearson r = 0.87 $R^2 = 0.76$ $p = 0.005$; $n = 8$). **I**–**L** Confocal images of the OV/MePO showing (**I**) the expression of P-nNOS along with the endogenous fluorescence of the FlincG3-cpEGFP protein upon an intraperitoneal injection of saline or kp-10 and (**L**) the expression of nNOS, GnRH and DAPI nuclear staining along with the endogenous fluorescence of the FlincG3-cpEGFP protein upon an intraperitoneal injection of saline or kp-10 (1 nmol). Magnifications on the right indicate representative examples of GnRH-positive cells showing FlincG3 activation (solid arrowheads) upon kp-10 administration. Values indicate means ± SEM. ns: non-significant, $p > 0.05$, $^{**}p < 0.01$. Source data are provided as a Source Data file. Schematic illustrations created in BioRender. *Chachlaki, K. (2026)* https://BioRender.com/*arnv9ca*. OV, organum vasculosum laminae terminalis. MePO, median preoptic nucleus. PAPA/NO, PAPA NONOate. kp-10, kisspeptin-10, NO, nitric oxide. P-nNOS, phosphorylated nNOS.

nNOS $^{OV/MePO}$ activation triggers surge-like LH release

According to the mathematical model we have previously proposed[26], the potential cumulative activation of nNOS$^{OV/MePO}$ neurons, such as we have shown to occur in the presence of kisspeptin, could result in the build-up of NO to levels capable of influencing neighboring GnRH neurons and synchronizing their activity. In order to assess whether the activation of nNOS$^{OV/MePO}$ neurons is sufficient to induce LH release, we stereotaxically delivered a viral vector carrying a designer receptor exclusively activated by designer drugs (DREADD), AAV-hSyn-DIO-hM3D(Gq)-mCherry, into the MePO of *Nos1cre* (*Nos1*^{cre}, B6.129-Nos1tm1(cre)Mgmj/J) female and male mice, allowing the selective expression of the activating DREADD hM3D(Gq) in nNOS$^{OV/MePO}$ neurons (Suppl. Fig. 3A, F). This approach provided an average efficiency of 77.8 ± 0.1% ($n = 4$) of nNOS$^{OV/MePO}$ neurons targeted with the activating DREADD, as indicated by RFP fluorescence (Fig. 3B). Tail blood was collected every 10 min for 180 min during diestrus in females, when nNOS$^{OV/MePO}$ activity is minimum. During the test, mice received an intraperitoneal injection of saline 5 min before the assessment of pulsatile LH release (min -5) and a CNO injection (1 mg/kg) to activate the DREADD at minute 65 or 105 (Suppl. Fig. 3B, G). As previously reported for intact female mice during diestrus, basal LH (0.25 ± 0.08 ng/ml) and the area under the curve (AUC) (25.0 ± 3.3 ng/ml), reflecting total LH output during the blood sampling protocol, were low, with mice displaying one pulse of LH over the first 60 min of blood sampling (Suppl. Fig. 3B). Interestingly, the selective activation of nNOS$^{OV/MePO}$ neurons upon CNO administration led to a significant increase in both basal LH (0.55 ± 0.1 ng/ml), and AUC (50.5 ± 6.4 ng/ml) levels (Suppl. Fig. 3C–E). Male mice displayed a comparable shift in LH secretory dynamics following nNOS$^{OV/MePO}$ neuron activation, with a clear transition from low-amplitude pulsatility to a prolonged elevation in circulating LH (Suppl. Fig. 3H–J), indicating that stimulation of nNOS$^{OV/MePO}$ neurons is sufficient to promote surge-like LH release in both sexes.

To determine whether this rise in LH secretion was mediated by NO, we repeated the same experimental paradigm in a separate group of female diestrous mice pre-treated with saline or the NOS inhibitor L-NAME (50 mg/kg), administered 30 min prior to tail bleeding (Fig. 3A). As expected, CNO administration elicited a marked increase in mean LH and AUC (Fig. 3C–G), with LH concentration continuing to rise up to 100 min post CNO injection (minute 180: 5.1 ± 1.5 ng/ml) (Fig. 3C). Strikingly, inhibition of endogenous NO synthesis significantly blunted this response (minute 180: 1.9 ± 0.2 ng/ml) (Fig. 3D–G), indicating that NO production by nNOS$^{OV/MePO}$ neurons is both necessary and sufficient to trigger an LH surge-like release.

Kisspeptin regulation of GnRH activity involves neuronal NO

NO/cGMP is a known regulator of the GnRH neuron excitability[27], and our results identify nNOS$^{OV/MePO}$ neurons as a source of endogenous NO-induced cGMP production in the vicinity of GnRH neurons. To evaluate the functional impact of manipulating the endogenous NO/cGMP pathway we performed electrophysiological recordings of GnRH neurons in the hypothalamus of female mice at diestrus and male mice following the pharmacological or genetic manipulation of the nNOS/NO signaling cascade, using a Nos1-deficient transgenic mouse line (*Nos1*$^{-/-}$). In agreement with our previous report showing elevated GnRH neuron firing in *Nos1*$^{-/-}$ mice during minipuberty (the early postnatal activation of the HPG axis)[16], spontaneous firing in GnRH neurons was also markedly increased in adult female *Gnrh*::*Gfp*; *Nos1*$^{-/-}$ mice at diestrus compared to their *Gnrh*::*Gfp*; *Nos1*$^{+/+}$ littermates (Suppl. Fig. 4A–C). This increased and sustained GnRH neuron firing was associated with a significantly reduced AUC and mean LH levels in both female and male *Nos1*$^{-/-}$ mice (Suppl. Fig. 5), in agreement with the hypogonadotropic hypogonadal phenotype associated with nNOS deficiency[16,28].

To further verify the hypothesis that local kisspeptin-nNOS interactions contribute to the regulation of GnRH neuron activity we examined kp-10 evoked GnRH neuron activity under our recording conditions. Bath or local application of kp-10 (10 nM) was able to stimulate GnRH neuron firing in hypothalamic slices from both *Gnrh*::*Gfp*; *Nos1*$^{+/+}$ and *Gnrh*::*Gfp*; *Nos1*$^{-/-}$ female diestrous and male mice (Fig. 4A, B, D, E and Suppl. Fig. 4D–G). Intriguingly, the ex vivo application of the NOS inhibitor L-NAME (1 mM), either before or after kp-10, resulted in an enhancement of the kp-10-induced increase in GnRH neuron firing (Fig. 4A, C and Suppl. Fig. 4D, E). Similarly, inhibition of sGC, the canonical NO receptor, with ODQ (10 µM) also increased the GnRH neuron firing rate, reinforcing the idea that NO acts through the NO–sGC–cGMP cascade to control the responsiveness of GnRH neurons to kisspeptin (Fig. 4A, C and Suppl. Fig. 4F, G). Conversely, the ex vivo bath application of an NO donor (DEA/NO; 100 µM) abolished this increase in the kp-10-induced response of GnRH neurons in *Gnrh*::*Gfp*; *Nos1*$^{-/-}$ mice, reducing the firing rate to that seen in *Gnrh*::*Gfp*; *Nos1*$^{+/+}$ mice upon kp-10 application (Fig. 4B, E). Similar results were obtained when impeding the degradation of endogenous cGMP through the administration of sildenafil, a selective PDE5 inhibitor, in *Gnrh*::*Gfp*; *Nos1*$^{-/-}$ mice (Fig. 4B, E), suggesting that cGMP accumulation can also regulate GnRH neuronal activity. Together, our results support a role for NO/cGMP signaling as a negative regulator of GnRH neuronal activity, fine-tuning the excitatory effects of kisspeptin via local NO production by nNOS$^{OV/MePO}$ neurons.

nNOS $^{OV/MePO}$ neurons modulate kisspeptin-driven LH release

Since, according to our results, kisspeptin promotes NO/cGMP production that in turn is required for the precise regulation of kisspeptin-induced GnRH neuronal activity, we focused our investigations on whether nNOS$^{OV/MePO}$ neuronal activity could itself be involved in the

https://doi.org/10.1038/s41467-026-69316-0

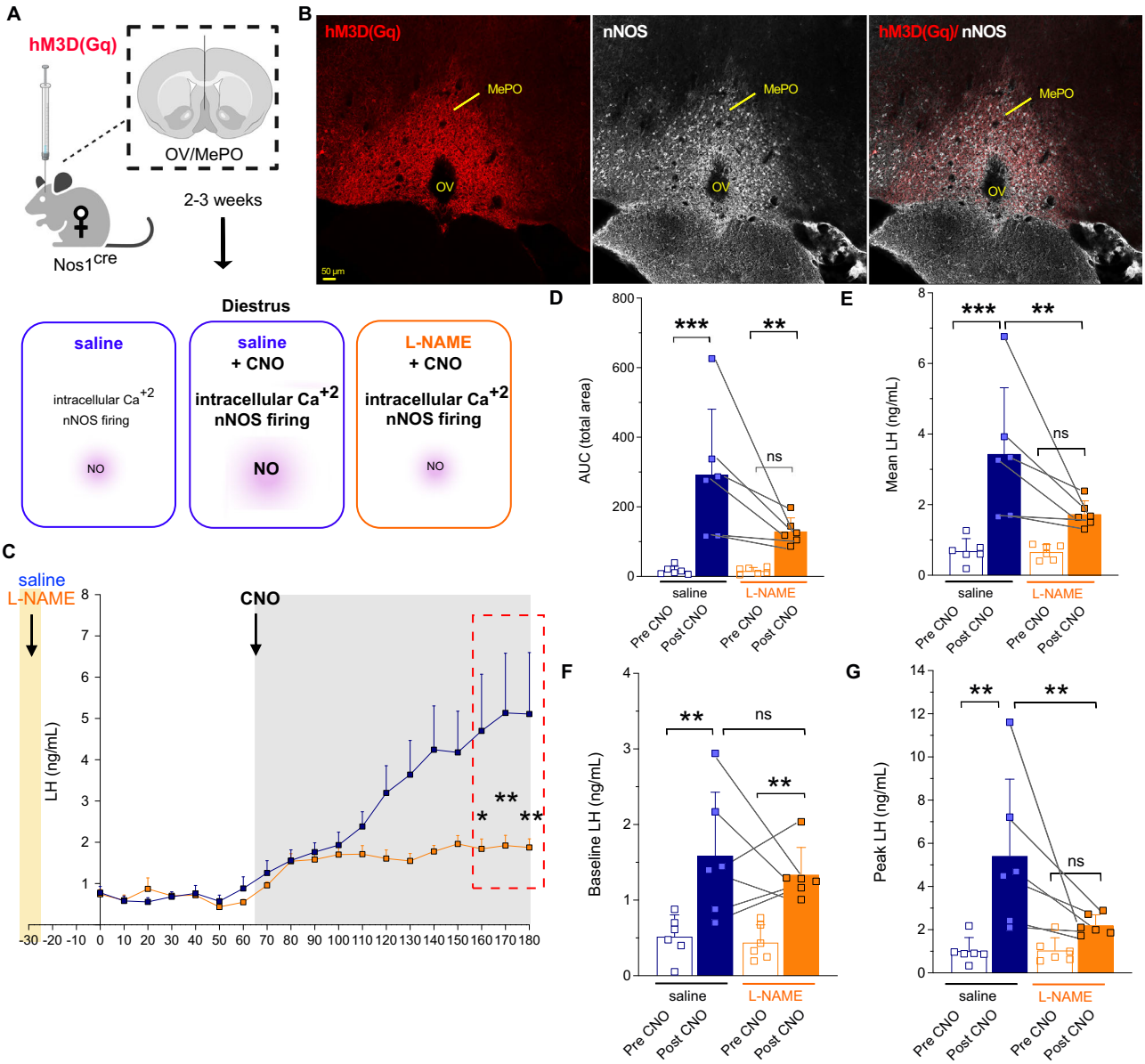

Fig. 3 | Endogenous NO production from nNOS$^{OV/MePO}$ neurons triggers a surge-like LH release pattern. A Graphical illustration of the strategy for the selective expression of AAV9-hM3D(Gq)-mCherry targeted to nNOS$^{OV/MePO}$ neurons in *Nos1^{cre}* female mice. **B** Confocal images show RFP, nNOS and colocalization immunoreactivity in the OV/MePO. **C** Graph of the LH release pattern over 180 min of serial blood sampling after administration of saline or L-NAME, 30 min before the beginning of the sampling. Arrow indicates the time of CNO administration (65th minute) (two-way ANOVA, Sidak's multiple comparisons test, time x treatment, $F_{(11, 110)} = 4.23$ $p < 0.001$; minute 160 $p = 0.03$, minute 170 $p = 0.009$, minute 180 $p = 0.008$; $n = 6$). Quantification of the **D** area under the curve (two-way ANOVA, Uncorrected Fisher's LSD, CNO effect: $F_{(1, 10)} = 24.18$ $p < 0.001$; saline pre CNO vs post CNO, $p < 0.001$; treatment effect: $F_{(1, 10)} = 4.48$ $p = 0.06$ post CNO saline vs L-NAME, $p = 0.008$; $n = 6$), **E** mean LH (two-way ANOVA, Uncorrected Fisher's LSD; CNO effect: $F_{(1, 10)} = 25.38$ $p < 0.001$; saline pre CNO vs post CNO, $p < 0.001$; treatment effect: $F_{(1, 10)} = 4.33$ $p = 0.06$; post CNO saline vs L-NAME, $p = 0.007$; $n = 6$), **F** basal LH (two-way ANOVA, Uncorrected Fisher's LSD, CNO effect: $F_{(1, 10)} = 25.84$ $p < 0.001$; saline pre CNO vs post CNO, $p = 0.003$; L-NAME pre CNO vs post CNO, $p = 0.008$; $n = 6$), and **G** peak LH (two-way ANOVA, Uncorrected Fisher's LSD, CNO effect: $F_{(1, 10)} = 16.45$ $p = 0.002$; saline pre CNO vs post CNO, $p = 0.001$; treatment effect: $F_{(1, 10)} = 3.87$ $p = 0.002$; post CNO saline vs L-NAME, $p = 0.007$; $n = 6$) levels of the *Nos1^{cre}* animals before and after CNO administration in saline and L-NAME injected animals. Experiment was independently repeated twice with similar results. Values indicate means ± SEM. ns: non-significant, $p > 0.05$, $^{*}p < 0.05$, $^{**}p < 0.01$, $^{***}p < 0.001$. Source data are provided as a Source Data file. Schematic illustrations created in BioRender. *Chachlaki, K. (2026)* https://BioRender.com/*arnv9ca*. 3 V, third ventricle. OV, organum vasculosum laminae terminalis. MePO, median preoptic nucleus. kp-10, kisspeptin-10. NO, nitric oxide. CNO, Clozapine N-oxide. AUC, area under the curve. LH, luteinizing hormone.

fine-tuning of kisspeptin-mediated LH release. To this end, we first injected the viral tool AAV-hSyn-DIO-hM4D(Gi)-mCherry carrying an inhibitory DREADD hM4(Gi)[29] into the MePO of *Nos1^{cre}* male mice to selectively target nNOS$^{OV/MePO}$ neurons. DREADD activation by CNO administration had no effect on the LH secretion pattern in either female or male mice, consistent with the very low basal activity of nNOS$^{OV/MePO}$ neurons under these conditions (Suppl. Fig. 6). Kp-10 was then intraperitoneally administered before and after CNO administration (Fig. 5A). As expected, the application of kp-10 (1 nmol) during basal nNOS$^{OV/MePO}$ neuronal activity (i.e., before CNO) elicited a rapid increase in LH release (peak LH = 2.8 ± 0.1 ng/ml) (Fig. 5B–G). Intriguingly, the inhibition of the nNOS$^{OV/MePO}$ population by CNO resulted in an enhanced kp-10-induced LH response (peak LH = 4.6 ± 0.5 ng/ml) (Fig. 3B–G), indicating that nNOS$^{OV/MePO}$ neurons provide inhibitory feedback to GnRH neurons, triggered specifically by kisspeptin activation. In agreement with this, the AUC (Fig. 5C), mean

https://doi.org/10.1038/s41467-026-69316-0

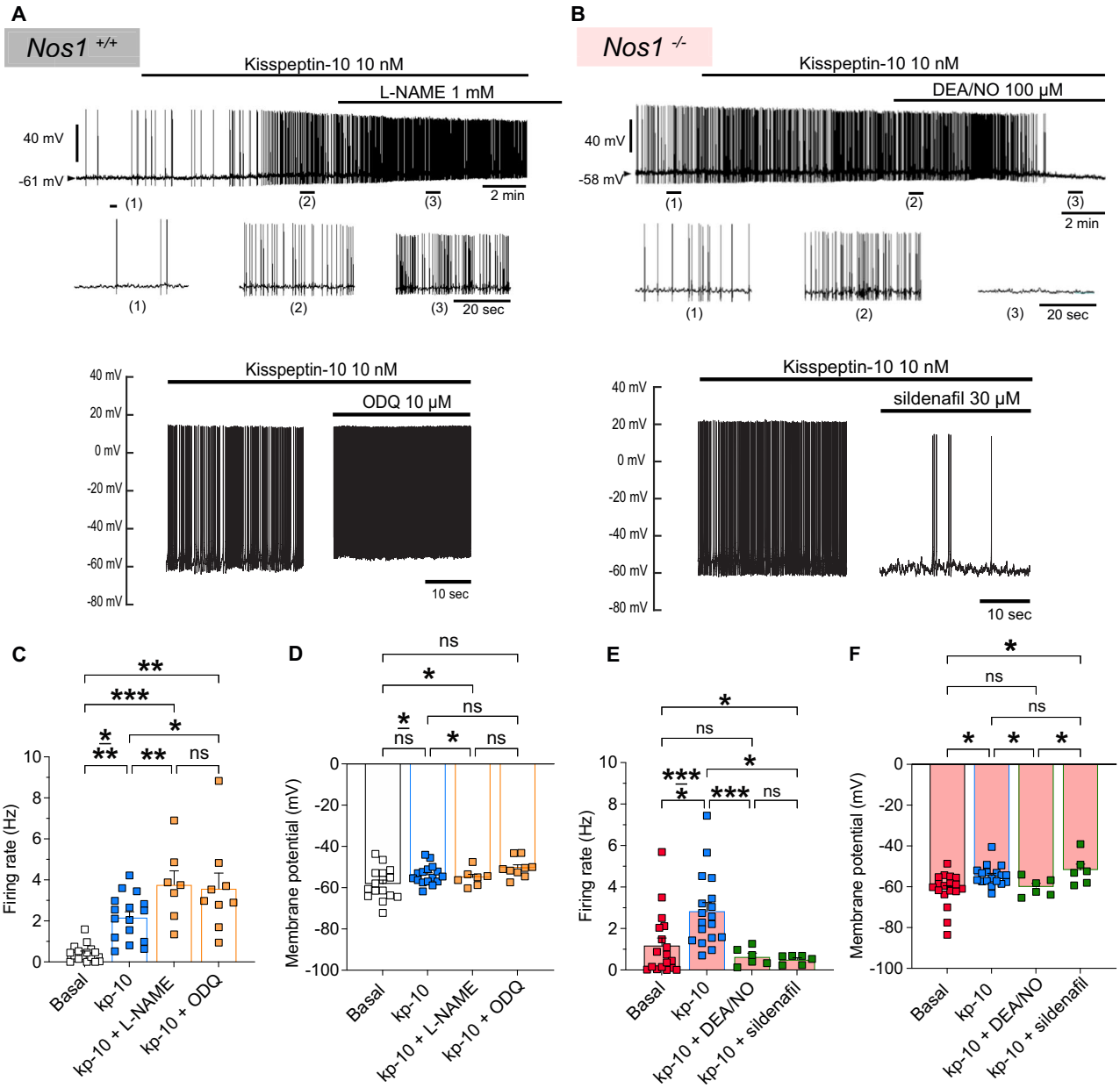

Fig. 4 | Canonical NO signaling controls GnRH neuronal activity in kisspeptin-excited GnRH neurons. A, **B** Representative whole-cell current-clamp recordings from a GnRH neuron of **A** a *Gnrh::Gfp Nos1*$^{+/+}$ mouse in the presence of bath application of kp-10 (10 nM) and the NOS inhibitor (L-NAME; 1 mM) or the sGC inhibitor (ODQ; 10 µM), **B** a *Gnrh::Gfp Nos1*$^{-/-}$ mouse in the presence of bath application of kp-10 (10 nM) and the NO donor DEA/NO (100 µM) or the phosphodiesterase 5 inhibitor sildenafil (30 µM). Bottom traces show expanded time-scales of the recording at the indicated time point 1, 2 and 3. (**C**–**F**) Since initial analyses revealed no difference between the sexes in the direction or magnitude of changes between basal values and kp-10 treatment, data from female and male mice were pooled for display; however, L-NAME and DEA/NO were applied only to females and ODQ and sildenafil only to males. **C** Spontaneous firing frequency (Wilcoxon two-tailed paired t-test basal vs. kp-10 $p < 0.001$; $n = 17$ cells, $n = 12$ mice; RM one-way ANOVA, Holm-Sidak's multiple comparison test, $F_{(2, 12)} = 20.70$, $p < 0.001$; basal vs. kp-10 plus L-NAME $p < 0.001$; kp-10 vs. kp-10 plus L-NAME $p = 0.007$; $n = 7$, $n = 6$ and $F_{(1.2, 11)} = 17.25$, $p = 0.001$; basal vs. kp-10 plus ODQ $p = 0.004$; kp-10 vs. kp-10 plus ODQ $p = 0.05$; $n = 10$ $n = 6$) and **D** membrane potential (Wilcoxon two-tailed paired t-test basal vs. kp-10 $p = 0.01$; $n = 17$ cells, $n = 12$ mice; RM one-way ANOVA, Holm-Sidak's multiple comparison test, $F_{(1.2, 7.3)} = 9.97$, $p = 0.01$; basal vs. kp-10 plus L-NAME $p = 0.05$; kp-10 vs. kp-10 plus L-NAME $p = 0.05$; $n = 7$, $n = 6$) in GnRH neurons from a *Gnrh::Gfp; Nos1*$^{+/+}$ diestrous female and male mice under basal conditions, in the presence of kp-10 and following the co-application of L-NAME (in females only) or ODQ (in males only); **E** spontaneous firing frequency (Wilcoxon two-tailed paired t-test basal vs. kp-10 $p < 0.001$; $n = 18$, $n = 8$; RM one-way ANOVA, Holm-Sidak's multiple comparison test $F_{(2, 16)} = 30.39$, $p < 0.001$; kp-10 vs. kp-10 plus DEA/NO $p < 0.001$ $n = 12$, 6 $n = 6$, 4 and test $F_{(1, 5.1)} = 10.32$, $p = 0.02$; basal vs. kp-10 plus sildenafil $p = 0.02$; kp-10 vs. kp-10 plus sildenafil $p = 0.05$; $n = 6$, $n = 2$) and **F** membrane potential (Wilcoxon two-tailed paired t-test basal vs. kp-10 $p < 0.001$; $n = 18$, $n = 8$; two-tailed unpaired t-test kp-10 plus DEA/NO vs. kp-10 plus sildenafil $p = 0.04$; RM one-way ANOVA, Holm-Sidak's multiple comparison test $F_{(2, 16)} = 7.19$, $p = 0.006$, kp-10 vs. kp-10 plus DEA/NO $p = 0.02$ and $F_{(1.1, 5.3)} = 15.23$, $p = 0.01$; basal vs. kp-10 plus sildenafil $p = 0.03$; $n = 6$, $n = 2$) of GnRH neurons recorded from *Gnrh::Gfp; Nos1*$^{-/-}$ diestrous female and male mice under basal conditions, in the presence of kp-10 and the co-application of DEA/NO (in females only) or sildenafil (in males only). Values indicate means ± SEM. ns: non-significant, $p > 0.05$, *$p < 0.05$, **$p < 0.01$, ***$p < 0.001$. Source data are provided as a Source Data file. kp-10, kisspeptin-10.

https://doi.org/10.1038/s41467-026-69316-0

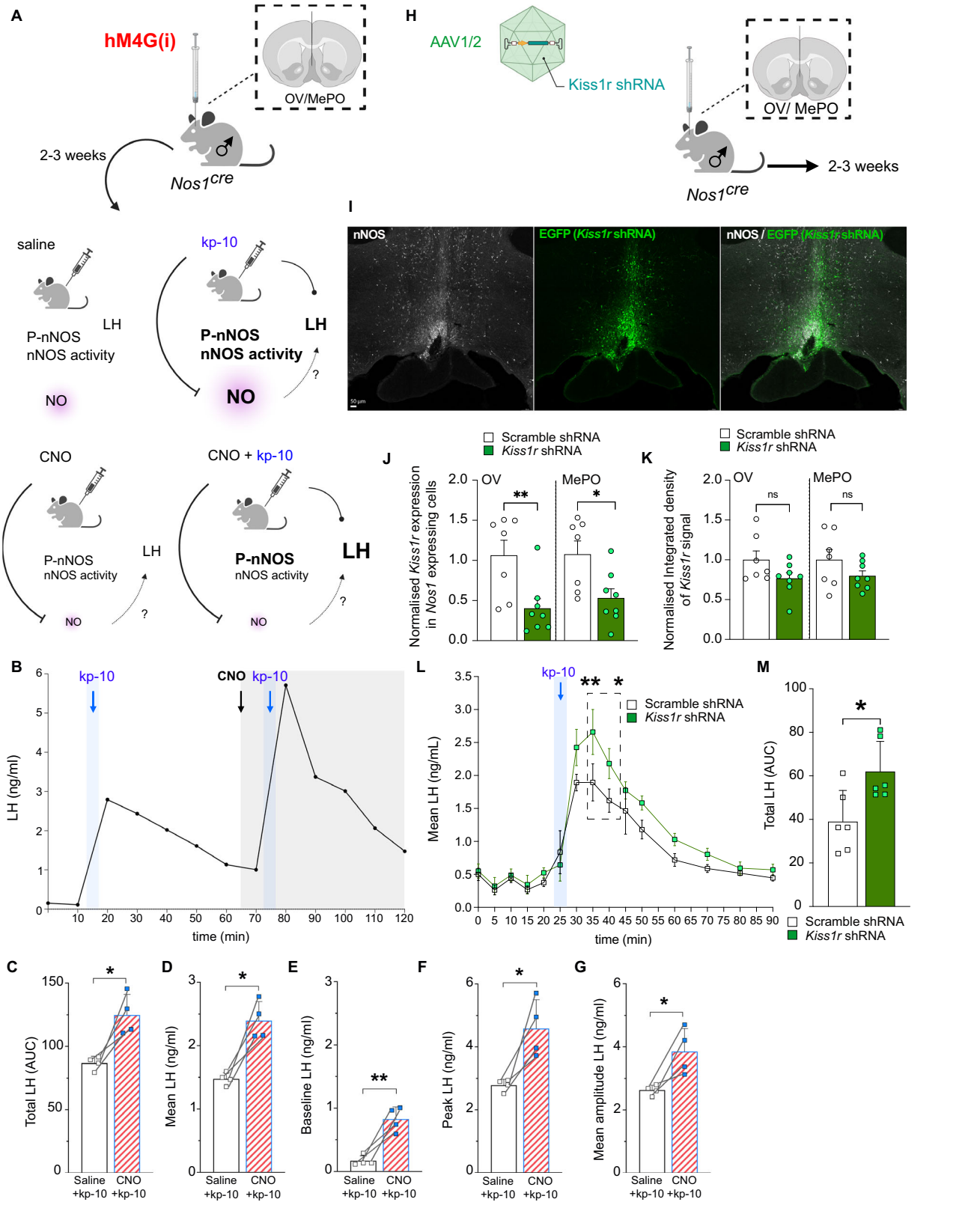

(Fig. 5D) and basal LH levels (Fig. 5E) were all increased in the presence of kisspeptin following CNO administration.

To specifically assess the role of kisspeptin signaling in nNOS$^{OV/MePO}$ neurons, we generated and injected an AAV expressing a Cre-dependent shRNA targeting *Kiss1r* into the OV/MePO of *Nos1*^{cre} mice (Fig. 5H, I). This strategy resulted in a ~60% reduction in *Kiss1r* expression specifically in nNOS neurons (Fig. 5J; Suppl. Fig. 7). The overall signal for *Kiss1r* in the OV/MePO trended towards a decrease, consistent with its selective loss from about half of the nNOS neurons, since ~40% of them normally express the receptor in Di/mE females and males, and with the relatively small percentage of *Kiss1r*-expressing cells that are also *Nos1* positive in this nucleus (Fig. 5K; Suppl. Fig. 7). Remarkably, the selective knockdown of *Kiss1r* reproduced the effect of nNOS$^{OV/MePO}$ neuron inhibition, as peripheral kisspeptin

Fig. 5 | nNOS $^{OV/MePO}$ neurons restrain kisspeptin-induced LH release via Kiss1r-dependent signaling. A Graphical illustration of intact *Nos1*^{cre} male mice injected into the MePO with the AAV-hSyn-DIO-hM4(Gi)-mCherry and intraperitoneally with kp-10 (1 nmol, 15th and 75th minute). **B** Representative LH pulse profile and analysis of **C** area under the curve (AUC) (two-tailed paired t-test $t_{(3)=}$ 5.07 $p = 0.01$; $n = 4$), **D** mean LH (two-tailed paired t-test $t_{(3)} = 6.64$ $p = 0.007$; $n = 4$), **E** baseline LH (two-tailed paired t-test $t_{(3)} = 5.89$ $p = 0.01$; $n = 4$), **F** peak LH (two-tailed paired t-test $t_{(3)} = 3.98$ $p = 0.02$; $n = 4$), and **G** mean amplitude of LH responses (two-tailed paired t-test $t_{(3)} = 3.98$ $p = 0.03$; $n = 4$) before or after CNO administration (65th minute). **H** Graphical illustration of the strategy for the selective expression of AAV1/2-CMV-DIO-shKiss1r(3x)-EGFP targeted to nNOS$^{OV/MePO}$ neurons in *Nos1*^{cre} male mice. **I** Confocal images show EGFP, nNOS immunoreactivity in the OV/MePO. **J**, **K** Quantification of **J** the percentage of cells positive for *Nos1* mRNA as well as *Kiss1r* mRNA in the OV and MePO (respectively, Mann-Whitney test, scrambled vs. shRNA: U = 6 $p = 0.009$; U = 9 $p = 0.03$; $n = 7, 8$) and of the (**K**) integrated intensity of the *Kiss1r* signal in the OV/MePO of mice injected with the scrambled or *Kiss1r* shRNA. **L** Representative LH pulse profile (mixed-effects analysis with Sidak's multiple comparisons test, Time x condition effect $F_{(14, 40)} = 2.44$ $p = 0.01$; minute 35 $p = 0.008$, minute 40 $p = 0.04$; $n = 6, 6$) and analysis of the **M** area under the curve (AUC) (Mann-Whitney test, scrambled vs. shRNA: U = 4 $p = 0.02$; $n = 6, 6$) of male mice injected with the scrambled or *Kiss1r* shRNA and receiving an intraperitoneal administration of kp-10 (20th minute). Values indicate means ± SEM. ns: non-significant, $p > 0.05$; * $p < 0.05$. ** $p < 0.01$. *** $p < 0.001$. Source data are provided as a Source Data file. Schematic illustrations created in BioRender. *Chachlaki, K. (2026)* https://BioRender.com/*arnv9ca*. OV, organum vasculosum laminae terminalis. MePO, median preoptic nucleus. kp-10, kisspeptin-10. NO, nitric oxide. AUC, area under the curve. LH, luteinizing hormone.

administration elicited an exaggerated LH surge (Fig. 5L, M), indicating that *Kiss1r*-dependent signaling in these neurons is required to restrain kisspeptin-induced LH release. These results, together with our electrophysiological data, strengthen the importance of nNOS$^{OV/MePO}$ neuron activity and their responsiveness to kisspeptin in the fine-tuning of GnRH neuronal firing and subsequent LH release.

Kisspeptin drives LH release via dual activation-inhibition by NO

In order to further explore the physiological significance of kisspeptin-NO interactions for the GnRH secretion profile, we assessed whether in vivo pharmacological manipulation of NO/cGMP signaling could modulate the kisspeptin-induced LH response. To this end, intact wildtype (WT) male mice were intraperitoneally administered saline, the NOS inhibitor L-NAME (50 mg/kg) or sildenafil (15 mg/kg), 30 min before blood sampling, and were then subjected to two kp-10 (1 nmol) administrations at an interval of one hour (Fig. 6A). Treatments did not modify basal LH levels prior to kp-10 administration (Fig. 6B). As expected, kp-10 administration induced a rapid, sharp increase in LH secretion in saline-treated animals. The administration of L-NAME did not impact the ability of kp-10 to efficiently stimulate GnRH/LH secretion, since, within 5 min of kp-10 administration, both groups had identical LH levels (Fig. 6F). However, in the absence of NO, the LH profile during the resolution phase was significantly altered. In agreement with what was seen upon pharmacogenetic inhibition of nNOS$^{OV/MePO}$ neurons, the administration of L-NAME induced an overshooting of the kisspeptin-induced LH response, which continued to rise even when LH values in saline-treated animals were rapidly decreasing (Fig. 6E), supporting the view that kisspeptin-induced NO release is necessary to end kisspeptin-induced GnRH/LH secretion. Interestingly, the administration of sildenafil, which prolongs the activity of the NO/cGMP cascade, led to a faster clearing of the kisspeptin effect, with LH levels eventually dropping below those in saline-treated animals (Fig. 6G). A second administration of kp-10, at the same dose as the initial one, 60 min later, resulted in a potentiated LH response to kisspeptin in animals treated with saline (Fig. 6F). Animals treated with L-NAME also displayed an enhanced LH response to the second kp-10 administration, similar to what was seen during the first kp-10 administration (Fig. 6E, F). Consistently, L-NAME treatment increased mean LH levels and AUC over the 180-min period (Fig. 6C, D). Intriguingly, sildenafil treatment, by amplifying the effects of endogenous NO through the inhibition of cGMP degradation, prevented the potentiation of LH release during the second administration of kp-10 compared to the first one, leading to an attenuated peak value of LH levels in comparison to the saline-treated animals (Fig. 6E, F). Of note, sildenafil treatment resulted in a faster decline in LH levels, with lower nadir levels at the end of the experiment (Fig. 6G). Similar experiments performed in female mice revealed the same response pattern, with L-NAME enhancing the kisspeptin-induced LH response, and sildenafil producing a mild constraining trend, with no measurable change, likely reflecting cycle-dependent saturation of cGMP signaling (Suppl. Fig. 8). Overall, our data support a role for NO/cGMP signaling in both amplification and resolution phases of the kisspeptin-induced LH response.

Discussion

The identification and characterization of both the positive and the negative regulators of the GnRH neural network is crucial for understanding the intricate balance of stimulatory and inhibitory signals that govern reproductive function. Kisspeptin is the most potent stimulator of GnRH activity, while neuronal NO acts on GnRH neurons as an inhibitory regulator (for review see refs. 8,14). Here we report that nNOS$^{OV/MePO}$ neurons express the *Kiss1r* mRNA, and that *Kiss1r* expression in these neurons is dynamically regulated across the estrous cycle, with the highest proportion of *Kiss1r*-expressing nNOS neurons observed in proestrus, as well as by sex, with males exhibiting expression levels comparable to those of diestrous females. Using state-of-the-art sensors, we show that kisspeptin enhances nNOS enzymatic activity to drive the production of NO from nNOS$^{OV/MePO}$ neurons in situ and that peripheral administration of kisspeptin or the chemogenetic manipulation of nNOS$^{OV/MePO}$ neurons fine-tunes LH release through a Kiss1r-dependent modulation of nNOS activity. Additionally, pharmacological approaches that either suppress or amplify kisspeptin-induced NO release indicate that kisspeptin uses highly diffusible NO to cap the amount of LH released and shut down the LH surge it triggers. Intriguingly, we observed a similar phenomenon at the cellular level, indicating that kisspeptin-GnRH signaling comprises a self-limiting step in the form of kisspeptin-induced NO production, which shapes and potentially curtails the excitatory response. This close relationship between nNOS and kisspeptin neurons and their ability to modulate GnRH activity in opposite ways supports the KiNG (Kisspeptin- nNOS-GnRH) neuronal network hypothesis, which indicates the existence of a kisspeptin- nNOS microcircuit of excitatory and inhibitory inputs coordinating GnRH/LH release. Indeed, deleterious mutations in the *KISS1* and *KISS1R* genes[4,30], and more recently *NOS1*[16], have all been found in patients with congenital hypogonadotropic hypogonadism, i.e., GnRH deficiency, supporting the importance of both kisspeptin and NO signaling in the control of fertility.

The expression of *Kiss1r* by non-GnRH neurons has been a matter of debate, possibly due to the low sensitivity of the techniques previously used to detect *Kiss1r* in these neurons[31]. However, the observation that the reinstatement of *Kiss1r* expression specifically in GnRH neurons of *Kiss1r*$^{-/-}$ mice is not sufficient to restore the LH response upon kisspeptin administration[32] supports the involvement of other, non-GnRH, Kiss1r-expressing cells in the shaping of the kisspeptin-induced LH release. This is in agreement with our data showing that peripheral kisspeptin administration induces a ~100% increase in the phosphorylation of the nNOS protein at Ser1412 and actually increases the local production of NO and cGMP in neurons surrounding the nNOS$^{OV/MePO}$ population. This aligns with the previously reported role

https://doi.org/10.1038/s41467-026-69316-0

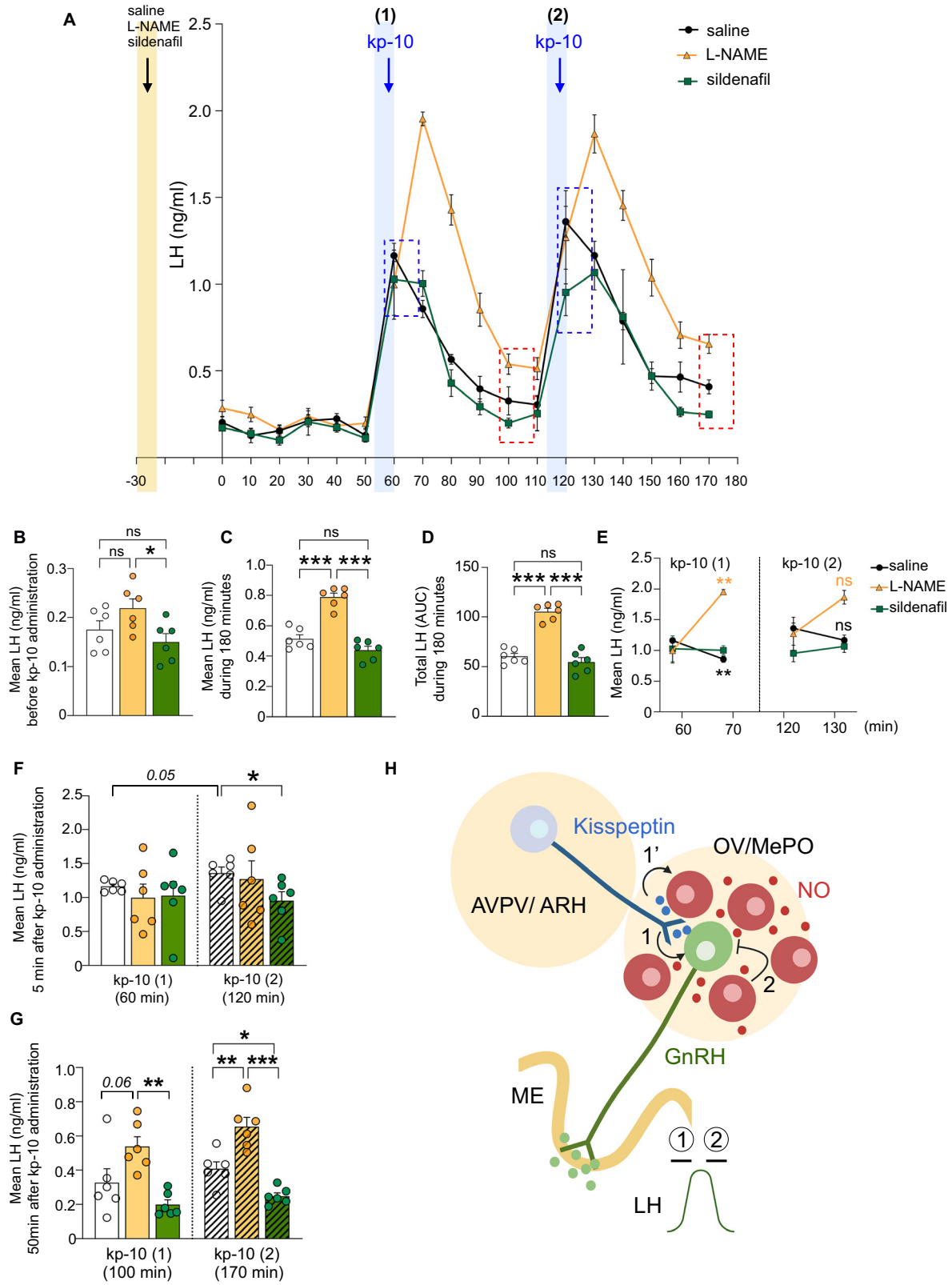

of Kiss1/Kiss1r in the mechanism driving the estradiol-promoted enzymatic activation of nNOS occurring on proestrus in the OV/MePO, correlating increased nNOS activity with the LH surge[17,21,22]. The ability of nNOS neurons to directly respond to kisspeptinergic signals in an estrogen-dependent manner supports the KiNG hypothesis, suggesting that GnRH release is ultimately determined by the equilibrium resulting from the interplay of NO and kisspeptin signaling across the estrous cycle. High estrogen levels during proestrus, by increasing AVPV kisspeptinergic inputs to nNOS$^{OV/MePO}$ neurons and thus promoting their enzymatic activation, could stimulate both nNOS and kisspeptin neurons, enabling the LH surge. Indeed, the knockdown of ERα in AVPV Kisspeptin (Kiss1^{AVPV}) neurons blunts the LH surge while maintaining LH pulsatile secretion[33,34], in agreement with the lack of effect of nNOS$^{OV/MePO}$ inhibition on the LH profile during diestrus (and

Fig. 6 | Effect of NO/cGMP signaling in the kisspeptin-induced LH response in male mice. A Mean LH pulse profiles of intact WT male mice after the administration of saline ($n = 6$), L-NAME ($n = 6$), or sildenafil ($n = 6$), 30 min before the beginning of blood collection. Kp-10 (1 nmol) was administered at min 55 and 115. **B** Mean baseline LH levels before administration of kp-10 (one-way ANOVA $F_{(2; 15)} = 3.80$, $p = 0.04$; sildenafil vs L-NAME $p = 0.04$; $n = 6$). **C** Mean LH (one-way ANOVA $F_{(2; 15)} = 58.10$, $p < 0.001$; saline vs. L-NAME $p < 0.001$; sildenafil vs. L-NAME $p < 0.001$; $n = 6$) and **D** area under the curve (AUC) for the total duration of 180 min (one-way ANOVA $F_{(2; 15)} = 58.10$, $p < 0.001$; saline vs. L-NAME $p < 0.001$; sildenafil vs. L-NAME $p < 0.001$; $n = 6$). **E** Comparison of mean LH levels 5 min vs. 10 min after the first (kp1; min 60 vs. min 70: two-tailed paired t-test saline $t_{(5)} = 5.83$ $p = 0.002$; L-NAME $t_{(5)} = 4.52$ $p = 0.006$; $n = 6$) and second (kp2; min 120 vs. min 130; two-tailed paired t-test: saline $t_{(5)} = 1.39$ $p = 0.22$; sildenafil $t_{(5)} = 0.56$ $p = 0.60$; L-NAME $t_{(5)} = 1.87$ $p = 0.12$; $n = 6$) kp-10 administration. **F** Mean LH levels 5 min upon first (kp1; min 60) and second (kp2; min 120) kp-10 administration (min 60 vs. min 120: two-tailed paired t-test saline $t_{(5)} = 2.45$ $p = 0.05$; min 120: two-tailed unpaired t-test saline vs. sildenafil $t_{(10)} = 2.53 = 0.03$; $n = 6$). **G** Mean LH response at washout upon the first (kp1; min 100) (one-way ANOVA $F_{(2; 15)} = 8.25$ $p = 0.004$, Tukey's post hoc test: saline vs. L-NAME, $p = 0.06$, sildenafil vs. L-NAME, $p = 0.003$; $n = 6$) and the second (kp2; min 170) (one-way ANOVA $F_{(2; 15)} = 25.1$ $p < 0.001$, Tukey's post hoc test: saline vs. sildenafil $p = 0.04$; saline vs. L-NAME, $p = 0.002$ sildenafil vs. L-NAME, $p < 0.001$, $n = 6$) kp-10 administration. **H** Graphical illustration explaining the possible mechanism behind the observed kisspeptin-NO interactions on the fine-tuning of GnRH/LH release. (1) Activation of the kisspeptin neurons of the AVPV and/or ARH drives GnRH/LH release by (1) acting on the GnRH neurons, while in parallel (1') stimulating NO release from $nNOS^{OV/MePO}$ neurons. (2) NO production in the vicinity of the GnRH neurons eventually inhibits GnRH neuron firing through the production of cGMP, thus ending the kisspeptin-induced response. Values indicate means ± SEM. ns: non-significant, $p > 0.05$; * $p < 0.05$. ** $p < 0.01$. *** $p < 0.001$. Source data are provided as a Source Data file. Schematic illustrations created in BioRender. *Chachlaki, K. (2026)* https://BioRender.com/ *arnv9ca*. kp-10, kisspeptin-10. AUC, area under the curve. LH, luteinizing hormone. NO, nitric oxide. AVPV, anteroventral periventricular nucleus. ARH, arcuate nucleus. OV, organum vasculosum laminae terminalis. MePO, median preoptic nucleus. ME, median eminence.

in male mice), and with previous studies suggesting that nNOS activity is dispensable for continuous/basal release but required for stimulated LH release[35].

According to our previously presented hypothesis, based on realistic mathematical modeling of the size and distribution of nNOS neurons in the OV/MePO[26], when the enzymatic activity of $nNOS^{OV/MePO}$ neurons is massively increased, NO concentrations could rise to levels capable of influencing neighboring GnRH neurons and synchronizing their activity. From our analysis, the number of active nNOS neurons under basal conditions is 57% lower than in the fully active state achieved after kisspeptin treatment. Accordingly, the model supports the idea that kisspeptin can switch the mode of operation of NO from a locally acting signal to a "volume transmitter" capable of influencing cells located at a distance. Yet, even though the stimulatory phosphorylation of nNOS at Ser1412 has been coupled with rapid NO production in vitro[24], such a mechanism had not been demonstrated in the hypothalamus in vivo. By generating a tool that enables measurement of NO/cGMP concentrations in vivo, we show that kisspeptin-induced nNOS phosphorylation is associated with massive NO/cGMP production in the OV/MePO of both sexes. This kisspeptin-induced NO production is additionally coupled with an increase in LH levels, supporting the view that highly diffusible NO is the perfect candidate to synchronize the widely dispersed GnRH neuronal population and enable the GnRH/LH surge. In support of this hypothesis, the pharmacogenetic activation of $nNOS^{OV/MePO}$ neurons during diestrus, i.e., when nNOS activity is at its nadir, was sufficient to provoke a proestrus-like LH surge, in agreement with previous studies showing that central NMDA administration can elicit LH release in *Kiss1*$^{-/-}$ and *Kiss1r* $^{-/-}$ mice, acting at least partially through nNOS neurons[36]. Importantly, this activation-induced LH surge was prevented by systemic administration of the NOS inhibitor L-NAME, indicating that the activation of $nNOS^{OV/MePO}$ neurons leads to NO release, and that this release is required to trigger the LH surge. Indeed, by demonstrating a paracrine action of NO and, importantly, cGMP production by GnRH neurons themselves, these findings reinforce the idea that NO is part of the mechanism modulating GnRH/LH release by acting downstream of kisspeptin, directly on GnRH neurons.

Previous studies had already provided evidence that NO could modulate GnRH neuronal activity via sGC-induced cGMP production[16,27]. Consistent with this, our electrophysiological recordings indicate that NO variations in the vicinity of GnRH neurons markedly influence GnRH excitability and shape the response to kisspeptin. Inhibition of NO synthesis with L-NAME amplified their response to kisspeptin, an effect that was reversible upon washout, revealing a dynamic interplay between local NO tone and kisspeptin signaling. Blockade of the downstream sGC pathway with ODQ produced a similar enhancement that persisted due to the irreversible nature of the inhibitor, whereas the pharmacological prolongation of cGMP signaling with sildenafil had the opposite effect, attenuating the kisspeptin-induced firing response, likely through residual NO/cGMP signaling by nNOSβ activity, which is still present in the *Nos1*$^{-/-}$ mouse in the absence of nNOSα[37], or by endothelial NOS. While these findings demonstrate that NO/cGMP exerts an inhibitory influence on GnRH neuron excitability, acting as a physiological restraint on kisspeptin-driven activation, this effect is not necessarily contradictory to the surge-like outcome of nNOS chemogenetic activation. Instead, the apparent stimulatory effect of $nNOS^{OV/MePO}$ activation could reflect a system-level consequence of transient inhibitory synchronization rather than direct excitation: by briefly silencing GnRH neurons, NO enables their synchronized reactivation once its levels decline. In contrast, after this activatory effect on GnRH neurons, the local diffusion of kisspeptin-induced NO release from $nNOS^{OV/MePO}$ neurons could engage a brake that ensures the GnRH system does not switch to a sustained, surge mode of GnRH/LH release (Fig. 7). In line with this concept, a recent study indicates that kisspeptin-NO interactions provide a mechanism for the modulation of the refractory period of GnRH neuronal activity[23]. This delicate balance within the KiNG network, between excitatory kisspeptin tone and the volumetric, paracrine action of NO in the vicinity of GnRH neurons, could thus maintain reproductive homeostasis. Such a mechanism for NO-mediated synchronization across a variable neuronal population could underlie the shifting GnRH neuron ensembles recently described during successive LH surges[37].

Supporting this model, the pharmacogenetic or pharmacological inhibition of $nNOS^{OV/MePO}$ neurons – via either direct silencing or systemic administration of L-NAME – abolished this inhibitory NO tone, leading to an amplified kisspeptin-stimulated LH response. Remarkably, selective *Kiss1r* knockdown in nNOS neurons phenocopied these effects, resulting in an exaggerated LH surge. These findings position Kiss1r-dependent signaling within $nNOS^{OV/MePO}$ neurons as a pivotal feedback element that restrains kisspeptin stimulation. Given that *Kiss1r* expression in these neurons fluctuates across the estrous cycle, peaking during proestrus, it likely participates in the dynamic tuning of GnRH/LH pulsatility, integrating hormonal state with hypothalamic network excitability. Importantly, NO blockade did not alter the ability of kisspeptin to directly promote the release of GnRH, but rather promoted a prolonged rise of LH levels in both sexes, suggesting an inefficient arrest of GnRH stimulation, similar to what has been previously shown upon the ablation of KNDy neurons in the rat brain[38]. Indeed, subsets of KNDy neuron afferents projecting to the preoptic area display oscillatory activity[39] and are closely apposed to both GnRH and nNOS neurons[40,41], raising the possibility that ARH neurons could

https://doi.org/10.1038/s41467-026-69316-0

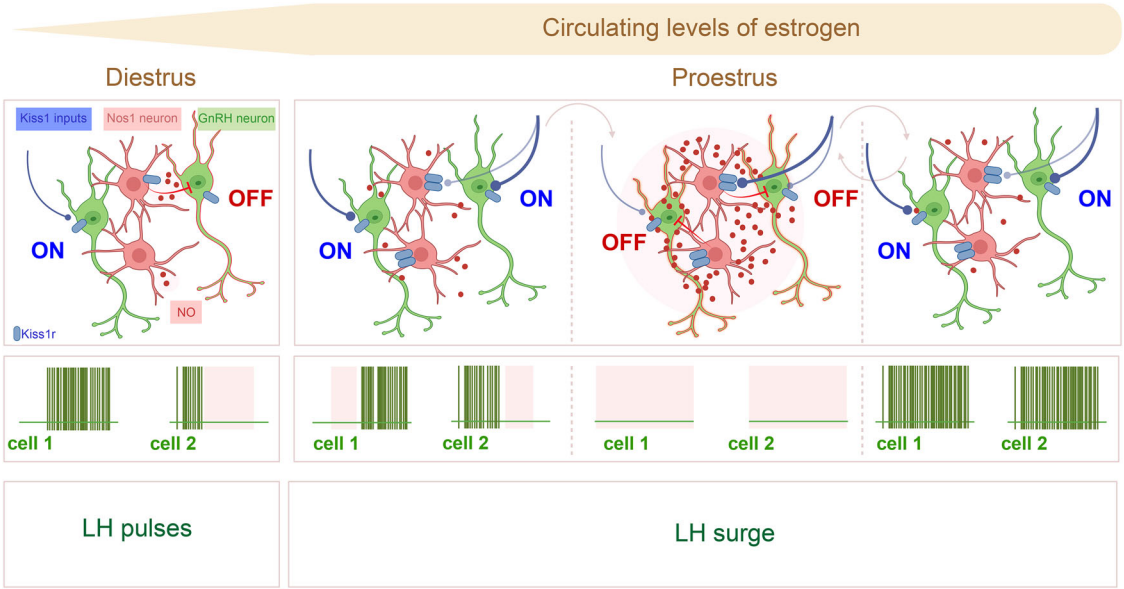

Fig. 7 | Proposed model of KiNG network dynamics across the estrous cycle. Diestrus: Kiss1 input activates GnRH neurons and weakly recruits nNOS$^{OV/MePO}$ neurons, which exhibit low *Kiss1r* expression at this stage. This results in low, spatially restricted NO/cGMP production that affects only GnRH neurons located near active nNOS cells. Local NO provides a limited inhibitory brake, sufficient to modulate kisspeptin-driven excitation but insufficient to synchronize GnRH neurons, which maintain dispersed rhythmic activity. Proestrus: Under high estrogen, kisspeptin input to GnRH neurons is strengthened, producing robust activation of individual GnRH neurons. However, this kisspeptin drive alone is not sufficient to align their activity, and the population remains asynchronous (left proestrus panel). In parallel, increased *Kiss1r* expression in nNOS$^{OV/MePO}$ neurons renders them strongly responsive to the same kisspeptin inputs. Their activation promotes NO volume transmission that transiently inhibits the scattered population of GnRH neurons, acting as a coordinated OFF signal (middle proestrus panel). As NO/cGMP levels decline, the coordinated release from inhibition drives a synchronized rebound in GnRH firing, consistent with the pattern required to initiate the preovulatory LH surge (right proestrus panel). Importantly, chemogenetic activation of nNOS$^{OV/MePO}$ neurons during diestrus is sufficient to reproduce this synchronized rebound, demonstrating that NO is a key organizing signal for GnRH neuron ensemble synchrony. Firing traces illustrate the transition from unsynchronized (direct kisspeptin excitation) to synchronized (NO-dependent coordinated inhibition) GnRH activity across the cycle. LH, luteinizing hormone. Schematic illustrations created in BioRender. Chachlaki, K. (2026) https://BioRender.com/*arnv9ca*.

contribute indirectly to the control of the nNOS$^{OV/MePO}$ population. In line with this, recent evidence shows that ARH Kisspeptin neurons switch from a peptide-driven "pulse generator" mode to a glutamatergic "surge-driving" mode under high estradiol, providing excitatory input to rostral Kiss1^{AVPV} neurons during the preovulatory phase[42].

In accordance with the ability of exogenous NO to induce a decrease in kisspeptin-induced GnRH firing, the administration of sildenafil in males, by triggering a gradual accumulation of cGMP around GnRH neuronal somata, abrogates the ability of kisspeptin to elicit a progressive increase in the magnitude of the LH response, a phenomenon previously reported in rats[43], eventually resulting in lower basal LH levels. Under these conditions, the first kp-10 administration would activate both GnRH neurons – hence inducing the secretion of GnRH from its nerve terminals – and nNOS$^{OV/MePO}$ neurons, resulting in NO-induced cGMP production and subsequently, GnRH neuron inhibition, terminating kisspeptin-induced LH secretion. In the presence of sildenafil, cGMP clearance would be limited, maintaining an enhanced inhibitory tone. A second kp-10 administration would thus occur on a background of sustained cGMP, with additional nNOS$^{OV/MePO}$ activation further amplifying this inhibitory tone, resulting in hyper-inhibition of GnRH neurons, negatively impacting LH secretion. Intriguingly, this effect was not observed in diestrous females, in which sildenafil had no significant impact on the kisspeptin-induced LH response. This apparent sex difference is unlikely to reflect a divergence in mechanisms, but rather, differences in basal NO tone or hormonal state across the estrous cycle. In diestrus, the first kp-10 administration may already drive the NO/sGC–cGMP pathway close to its inhibitory ceiling, leaving little dynamic range for further prolongation by PDE5 inhibition. Under these conditions, NO availability—rather than PDE5-dependent cGMP clearance—appears to set the inhibitory tone. Although we did not directly assess the impact of NO signaling on the intrinsic GnRH pulse generator, our data reveal a mechanism by which NO can shape the temporal structure of GnRH/LH output. KNDy neurons provide the endogenous rhythmic drive for pulsatile GnRH secretion, and their oscillatory input ultimately converges onto GnRH neurons. By dynamically modulating GnRH neuron excitability in response to kisspeptin, NO/cGMP signaling could influence how reliably each KNDy-derived burst is translated into a secretory event. In this framework, low NO levels during diestrus would maintain GnRH neurons in a permissive excitability range compatible with rhythmic activation, whereas high NO output during proestrus could facilitate the transient synchronization of GnRH neurons and the shift from recurrent, pulse-like activation toward a more sustained, surge-like mode.

In this framework, the nNOS-kisspeptin communication network emerges as a key integrative node in which hormonal state, Kiss1r-dependent signaling and NO/cGMP dynamics converge to balance excitation and inhibition within the hypothalamic reproductive circuit. Recent studies further highlight the translational relevance of this pathway: restoring hypothalamic NO signaling rescues reproductive function in preclinical models of polycystic ovary syndrome[29], and impaired NO transmission has been linked to female sexual dysfunction[44]. The physiological relevance of this pathway extends beyond the adult cycle. Notably, perinatal sildenafil in *Nos1*$^{-/-}$ mice has been shown to normalize GnRH system activity during minipuberty and mitigate later reproductive and cognitive comorbidities[16], underscoring NO–cGMP control as a developmental determinant of GnRH/LH dynamics and highlighting the therapeutic potential of targeting this pathway to complement kisspeptin-based approaches across developmental and adult reproductive disorders.

In summary, our study provides evidence supporting the involvement of the KiNG neuronal network in shaping the GnRH/LH release pattern. According to this model, during the estrogen negative feedback phase in diestrus, the activation of KNDy neurons results in kisspeptin release, stimulating GnRH secretion. In parallel, $nNOS^{OV/MePO}$ neurons directly sense kisspeptin signals in a tightly regulated manner due to the differential expression of *Kiss1r*. The resulting fine-tuning of nNOS enzymatic activity by kisspeptin allows, during the negative feedback phase, the production of low levels of NO/cGMP in the vicinity of GnRH neurons, indispensable for physiological GnRH neuronal activity, in part by switching off kisspeptin-induced GnRH/LH production and allowing the GnRH system to return to baseline. During the positive feedback phase, the activation of $Kiss1^{AVPV}$ neurons would result in kisspeptin being released around the $nNOS^{OV/MePO}$ population which, being more sensitive to kisspeptin due to increased *Kiss1r* expression, becomes maximally activated. This results in a substantial release of NO/cGMP, likely facilitating the synchronization of GnRH neuronal activity within the reach of this NO wave. The direct actions of kisspeptin on GnRH production/release and its indirect actions through NO could thus be two sides of the same coin, acting as the ON and OFF signals to fine-tune GnRH neuronal activity and initiate the LH surge. Aside from their potential physiological relevance, our current results further contribute to the hypothesis that NO could be the long-missing key to the synchronization of GnRH neurons.

Methods

Animals

Experiments were performed on adult (3-4 months old) male and female C57BL/6 J mice (Charles River Laboratories), *Nos1*^{cre} mice (B6.129-Nos1tm1(cre)Mgmj/J), *Nos1*-deficient (B6.129S4-Nos1tm1Plh/J) mice and *Gnrh::Gfp* mice (a generous gift of Dr. Daniel J. Spergel, Section of Endocrinology, Department of Medicine, University of Chicago, IL). *Nos1*$^{-/-}$*;Gnrh::Gfp* mice were generated in our animal facility by crossing *Nos1*$^{-/+}$ mice with *Gnrh::Gfp* mice. All mice were housed under specific pathogen-free conditions in a temperature-controlled room (21-22 °C) with a 12 h light/dark cycle and an average humidity of 42%. Mice had ad libitum access to food and water. Animal studies were approved by the Institutional Ethics Committees for the Care and Use of Experimental Animals of the Universities of Lille and the University of Geneva; all experiments were performed in accordance with the guidelines for animal use specified by the European Union Council Directive of September 22, 2010 (2010/63/EU) and were approved by the French Department of Research (APAFIS#2617-2015110517317420v5; APAFIS#29172-2020121811279767v5) and the State of Geneva (License number 369).

Pharmacological agents

Synthetic kisspeptin-10 [rodent metastin (45–54) amide; YNWNSFGLRY-NH2] was purchased from GeneCust and administered at 1 nmol per animal in vivo, or at 10 nM ex vivo. The NOS inhibitor Nω-Nitro-L-arginine methyl ester hydrochloride (L-NAME, Sigma #N5751; 50 mg/kg in vivo, 1 mM ex vivo), the cGMP-specific PDE5 inhibitor Sildenafil citrate (Sildenafil, Sigma-Aldrich #SML3033; 15 mg/kg in vivo, 30 µM ex vivo), and the Dimethyl Sulfoxide (DMSO, Millipore #317275) were purchased from Merck Life Science (Milano, IT). The selective inhibitor of NO-sensitive guanylyl cyclase 1H-[1,2,4]oxadiazolo[4,3-a]quinoxalin-1-one (ODQ, #0880; 10 µM) and Clozapine N-oxide dihydrochloride (CNO, # 6329; 1 mg/kg) were purchased from Tocris Bioscience (Bristol, UK). The NO donors (Z)-1-[N-(3-ammoniopropyl)-N-(n-propyl)amino]diazen-1-ium-1,2-diolate] PAPA/NONOate, # ALX-430-016; 5 µM) and the DEA/NO, 2-(N, N-diethylamino)-diazenolate-2-oxide.diethyl-ammonium salt (DEA NONOate, # ALX-430-034; 100 mM) was from Enzo Life Sciences (Exeter, UK).

Stereotaxic injections

The AAV9 hM4D DREADD (AAV-hSyn-DIO-hM4D(Gi)-mCherry) (Addgene; 44362-AAV9), the AAV9 hM3D DREADD (AAV-hSyn-DIO-hM3D(Gq)-mCherry) (Addgene; 44361-AAV9) and the AAV1/2 *Kiss1r* shRNA or Scrambled shRNA (AAV-CMV-DIO-shKiss1r(3x)-EGFP, # P210901-1002gjb; AAV-FLEX-shScramble-EGFP, # VB220803-1150vgq, VectorBuilder) were stereotaxically injected into the OV/MEPO of *Nos1*^{cre} female and male mice after dilution in PBS to reach a titer of 4.5×10^{12} vg/mL. The AAV9 FlincG3 (AAV-CMV-FlincG3) (titer = 10×10^{12} vg/mL; Genecust) was stereotaxically injected into the OV/MEPO of wild-type female mice. Animals were kept under general anesthesia (induction 4% in air 2 L/min, then 1.5% in air 0.3 L/min), after local injection of lidocaine (30 microliters of a 0.5% solution, s.c.) and pre-emptive Meloxicam treatment (5 mg/kg). The needle of a 2 µL Hamilton Neuros syringe (Hamilton; catalog # 65459-01) was placed into the target region. After 5-min, 300 nL of the solution containing viral particles was delivered at a rate of 80 nL per minute. 10 minutes after the completion of the delivery, the needle was slowly removed, and the skin was sutured. To target the OV/MEPO, the following coordinates were used: anterior-posterior (A-P) = + 1.3 mm; medial-lateral (M-L) = 0 mm; dorsal-ventral (D-V) = - 4.8 mm.

Mice were allowed to recover for three weeks after brain surgery to ensure sufficient viral transduction. Following the in vivo experiments, all animals were sacrificed and the brains were processed for immunohistochemistry to verify the efficiency and specificity of viral expression. Animals in which the infection covered less than one-third of the OV/MePO were excluded from the analysis. The average transduction efficiency and off-target infection rate were determined by counting nNOS-labeled neurons, RFP (mCherry) /GFP-positive neurons, and double-labeled cells within a manually defined subregion of the OV and MePO for each animal. To validate the downregulation of the kisspeptin receptor, an independent cohort of mice was injected with AAV *Kiss1r* shRNA or scrambled shRNA, and brains were processed for fluorescence in situ hybridization as described below.

Examination of physiology

Adult female mice (3–6 months of age) were examined daily for two consecutive estrous cycles to confirm regular cycling before use in experiments. Vaginal smears were collected and analyzed under a light microscope to determine the stage of the estrous cycle, and all experimental procedures were performed on the indicated day of the cycle.

Assessment of LH secretion dynamics and LH assay

In this study, LH release was used as a physiological readout of hypothalamic GnRH output, consistent with previous work demonstrating that pituitary LH secretion faithfully reflects changes in GnRH neuronal activity and release dynamics. For the pulsatility test, mice were habituated to handling and tail-tip blood sampling for at least 10 days prior to the experiment. When a viral vector was administered stereotaxically, animals were allowed to recover for two weeks before the start of habituation. Blood samples for measuring circulating LH concentrations were collected in the morning and, for females, only during the diestrus stage. Mice were gently restrained, and tail-tip blood was sampled at 5- or 10-minute intervals, as indicated in the figure legend. For each time point, 4 µL of whole blood were collected into Eppendorf tubes preloaded with 56 µL of 0.01 M PBS containing 0.05% Tween-20 and 0.2% BSA, thoroughly mixed, and kept on ice until storage at −80 °C. LH concentration was measured using a highly sensitive Enzyme-linked Immunosorbent Assay (ELISA) recently described in Kreisman et al.[45] . Briefly, we used a 96-well high-affinity binding microplate (Corning) coated with 50 µL of primary capture antibody (bovine LHβ subunit, 518B7; L. Sibley; University of California, UC Davis) diluted at 1 µg/ml in 0.01 M PBS. The mouse LH-RP was provided by Dr. Albert F. Parlow (National Hormone and Pituitary

Program, Torrance, California, USA) and used to generate a standard curve with a twofold serial dilution. The detection primary antibody (Mouse Monoclonal LH antibody, cat: Medix, 5303 SPRN SPRN-5) was biotinylated using the EZ-Link NHS-PEG4 Biotinylation Kit (Thermo Scientific, catalog No. PI21455) and used at a concentration of 1μg/ml, diluted in 0.01M PBS-0.05%Tween, 5 % skim milk powder. For the final step, the poly-HRP Streptavidin (Thermo Fisher, Cat# N200) was diluted 1:8000 in 0.01M PBS-0.05% Tween, then revealed with 100 µL of 1-Step Ultra TMB-ELISA Substrate Solution (Thermo Fisher Scientific, cat. #34028). The colorimetric reaction was stopped with stop solution of 50 µL of 3 M HCl. Optical density (OD) was read at 490 nm and 650 nm for background subtraction.

Fluorescence in situ hybridization

FISH was performed on frozen brain sections of 3-month-old female mice with the RNAscope Multiplex Fluorescent Kit v2 (323100, Advanced Cell Diagnostics). Estral cyclicity was assessed during 2 weeks by daily vaginal smears. Animals were anesthetized with isoflurane and then sacrificed by decapitation in the late afternoon of the first day of diestrus or proestrus. Brains were dissected and included in OCT medium (Tissue-Tek), frozen on dry ice, and stored at −80 °C until sectioning, while the edematous swelling of the uterus was visually checked to confirm the estrous stage. Tissues were cryosectioned (Leica cryostat) coronally at 16 µm on Superfrost Plus slides and stored at -80 °C. Sections were processed according to the manufacturer's protocol, using specific probes to detect *Nos1* (437651-C2, NM_008712.2, target region 2-1097), *Kiss1r* (408001, NM_053244.5, target region 21 – 1599), *Kiss1* (476291, XM_006529679.2, target region 121-1376) and *Gnrh1* (476281-C3, XM_006518564.3, target region 81-914) mRNAs. Hybridization with a probe against the Bacillus subtilis dihydrodipicolinate reductase (DapB) gene (320878) was used as a negative control.

RNAscope preparations were analyzed on the LSM 710 Zeiss confocal microscope. Excitation wavelengths of 405/443 nm, 488/518 nm, 561/699, and 633/699 were selected to image the different channels. All images were taken with the objective EC Plan-Neofluar M27 (thread type) using the 40X oil objective with a numerical aperture of 0.50, and a zoom of 1.4. Z-stack images were taken every 1 µm, for a total of 10 µm per section. All the images are presented as maximal intensity projections (MIP) of three-dimensional volumes along the optical axis. Images to be used for figures were pseudocolored and adjusted for brightness and contrast using Photoshop (Adobe Systems, San Jose, CA).

Cell counting. The nomenclature of brain regions used in this article and the definition of the region of interest was based on the ones described in the Allen brain atlas[46]. The cell counts were undertaken unilaterally on maximal intensity projections (MIP) images. For each mouse, the number of single-labeled *Nos1* positive, *Kiss1* positive and *Kiss1r*-positive neurons, and double-labeled *Nos1/Kiss1r* and *Nos1/Kiss1* neurons in the region of the OV/MePO (represented by plate 50 of the Allen Mouse Brain Atlas) and in the region of the AVPV (plate 53) were performed manually. To count DAPI nuclear staining, accounting for the total number of cells in the area, the particles were automatically counted on the images after binarization and segmentation using ImageJ. The representation of the percentage of *Nos1*, *Kiss1* and *Kiss1r* mRNA positive cells in the region was obtained by normalizing over the DAPI nuclear staining in the areas of interest.

Immunohistochemistry

Tissue preparation. Mice were anesthetized with a lethal dose of pentobarbital (DOLÉTHAL®, 5 mg/kg) and locally treated with Lidocain (30 µl of a 0.5% solution). Animals were perfused thoroughly with cold saline, until exsanguination, then perfused with cold fixative solution [4% paraformaldehyde (PFA), in 0.1 M PB, pH 7.4]. The brain was extracted and post-fixed with the same fixative solution for 2 h at 4 °C, then cryoprotected in PB 0.1 M 20% sucrose for 24 h at 4 °C. Afterwards, the brain was embedded in OCT medium (Tissue-Tek), frozen on dry ice, and stored at −80 °C until sectioning. Tissues were cryosectioned (Leica cryostat) coronally at 35 µm (free-floating sections).

Antibodies. The goat polyclonal anti-nNOS antibody (1:1000; Cat# OSN00004G, Lot#VF3001511) and the rabbit polyclonal anti-Ser1412 phospho-nNOS antibody (1:500; Cat# PA1-032, Lot#XE350390) were purchased from ThermoScientific. The rabbit polyclonal anti-RFP was purchased from Rockland (1:1000; Cat# 600-401-379). The rat polyclonal anti-GnRH (1:2500; Cat# EH1044) was a generous gift from Professor Hrabovszky (Laboratory of Reproductive Neurobiology, Institute of Experimental Medicine, Budapest, Hungary). The chicken polyclonal anti-GFP (1:1000; Cat# GFP-1020) was purchased from Aves Lab. The secondary antibodies were all purchased from Invitrogen and used at a final concentration of 1:500. Alexa Fluor 647-conjugated donkey anti-goat (1:500; Cat# A21447) was used for nNOS, and 568-conjugated donkey anti-rat (1:500; Cat# A78946) for GnRH immunolabeling. Alexa Fluor 568-conjugated donkey anti-rabbit (1:500; Cat# A10042) was used to detect phospho-nNOS and RFP (mCherry) expression, and the Alexa Fluor 488-conjugated donkey anti-chicken (1:500) was used to amplify the GFP expression of the *Kiss1r* shRNA/Scrambled vector.

Immunolabeling. Sections were washed 3 times for 5 min each in PB 0.1 M and then incubated in blocking solution (5% NDS, 0.3% Triton X-100 in PB 0.1 M) for 1 hour at room temperature. Sections were incubated for 48–72 h at 4 °C with the primary antibodies diluted in blocking solution, then rinsed 3 times for 5 min each in PB 0.1 M. The sections were incubated with secondary antibodies diluted in PB 0.1 M for 1 h at room temperature, then rinsed in PB 0.1 M 3 times for 5 min each, and finally incubated 7 min with DAPI (1:5000 in PB 0.1 M) for nuclear staining. After washing, sections were mounted on glass slides and coverslipped under Mowiol medium.

Digital image acquisition. Images were acquired using a Leica Stellaris 5 confocal microscope. Excitation wavelengths of 405, 488, 561, and 633 nm were selected to image the different channels. The images were acquired with a 20x/0.8 objective (numerical aperture NA = 0.80) with a zoom of 1.0. Z-stack images were taken every 1 µm, for a total of 20 µm per section. All images are presented as maximal intensity projections (MIP) of three-dimensional volumes along the optical axis. Images to be used for figures were adjusted for brightness and contrast using Photoshop (Adobe Systems, San Jose, CA).

Cell counting. The quantification of nNOS neurons co-expressing P-nNOS was undertaken by counting the number of single-labeled nNOS-positive neurons and double-labeled nNOS/P-nNOS in the OV, represented by plate 50 of the Allen Mouse Brain Atlas. Cell counts were carried out unilaterally, represented as the percentage of nNOS neurons positive for P-nNOS immunoreactivity, and the values from each mouse were averaged to determine mean counts and SEM for each group. FlincG3 fluorescence was quantified by analyzing the integrated density. Using ImageJ analysis software, a region of interest of identical size was defined on every image in the region of the OV/MEPO, represented by plate 50 of the Allen Mouse Brain Atlas. The defined region was binarized, and the integrated intensity was then calculated for each image, which reflects the total number of pixels in the skeletonized image. In the same region of interest, the single-labeled nNOS-positive neurons and the double-labeled nNOS/FlincG3 neurons were also manually quantified. All values are presented as the averaged values from each mouse to determine mean counts and SEM for each age group.

Live FlincG3 imaging

Brain slice preparation. FlincG3 recordings were performed on acute brain slices from 8–12-week-old male mice. Animals were anesthetized with isoflurane and decapitated, and the brains were rapidly removed and placed in ice-cold artificial cerebrospinal fluid (aCSF) containing (in mM): NaCl 120, KCl 2, $NaHCO_3$ 26, KH_2PO_4 1.18, $MgSO_4$ 1.19, glucose 11, and $CaCl_2$ 2, continuously bubbled with 95% O_2 / 5% CO_2. Coronal slices (200 μm) encompassing the preoptic area were cut using a VT1200 vibratome (Leica). Slices were transferred to a recovery chamber containing oxygenated aCSF and maintained at 34 °C for 1 h, then allowed to cool to room temperature (≈22 °C) before imaging.

Live recording. Slices were placed in a 500 μL recording chamber mounted on an inverted microscope (Zeiss Axiovert 135TV, Carl Zeiss, UK) and superfused continuously (1.5 mL min^{-1}) with pre-warmed (37 °C) recording solution containing (in mM): NaCl 140, KCl 2, KH_2PO_4 1.18, glucose 5.5, HEPES 10, and $CaCl_2$ 1.5 (pH 7.4; 285–290 mOsm kg^{-1}). The solution was equilibrated with pure O_2 and supplemented with superoxide dismutase (100 U mL^{-1}). Imaging was performed using a Zeiss Axio Observer Z1 equipped with an Orca LT camera (Hamamatsu) and a 20× air objective (NA 0.8, Zeiss), under control of Zen Imaging Software (Zeiss). FlincG3 fluorescence was excited at 495 nm and collected at 519 nm. Exposure time was 300 ms, and illumination intensity was set to 30%. All pharmacological compounds were administered by superfusion.

Fluorescence data analysis. Fluorescence measurements were background-corrected and displayed as the change in intensity relative to the baseline divided by the baseline intensity (ΔF/F0) in Image-Pro Premier (version 9.1, MediaCybernetics). As appropriate, traces were corrected for NO-independent, post-NMDA undershoots and baseline drift[47] in Origin (version 10.1, OriginLab Corp., Northampton, MA). Results are given as means ± S.E. Each experiment was performed on a separate brain slice and repeated at least twice to ensure reproducibility; n values refer to the number of responders.

Electrophysiology

Brain slice preparation. Electrophysiological recordings were performed on acute brain slices obtained from 8–12-week-old female and male mice. Animals were anesthetized with isoflurane and decapitated, and the brains were rapidly removed and placed in ice-cold artificial cerebrospinal fluid (aCSF). Coronal slices (200–250 μm) containing the preoptic area were cut using a VT1200 vibratome (Leica). For Protocol 1, the aCSF composition was (in mM): NaCl 120, KCl 3.2, NaH_2PO_4 1, $NaHCO_3$ 26, $MgCl_2$ 1, $CaCl_2$ 2, and D-glucose 10 (300 mOsm, pH 7.4). For Protocol 2, the aCSF contained (in mM): NaCl 124, KCl 3, $CaCl_2$ 2, $MgSO_4$ 1.3, $NaHCO_3$ 26, NaH_2PO_4 1.25, and D-glucose 10 (300 mOsm, pH 7.4). All solutions were continuously bubbled with 95 % O_2/5 % CO_2 for at least 1 h before use. Slices were incubated in oxygenated aCSF at 34 °C (Protocol 1) or 37 °C (Protocol 2) for 1 h to recover, then maintained at room temperature until patch-clamp recording.

Patch-clamp recording. Individual coronal brain slices containing the preoptic area were transferred to a submerged recording chamber (Warner Instruments) and continuously perfused with oxygenated artificial cerebrospinal fluid (aCSF; 95% O_2/5% CO_2) at a rate of 2–3 mL/min. The bath temperature was maintained at 32.8 °C using a TC-344C temperature controller (Warner Instruments). GnRH neurons were visualized under 10× and 40× objectives using an upright fluorescence microscope equipped with infrared differential interference contrast optics (DM-LFSA, Leica) and an ORCA-Flash4.0 digital CMOS camera (Hamamatsu). Additional recordings were obtained with an LNscope (Luigs & Neumann) equipped with a BX51 fluorescence tower (Olympus) and an ORCA-Fusion camera (Hamamatsu). Recording pipettes (resistance 6–8 MΩ) were pulled from borosilicate glass capillaries (1.5 mm outer diameter, 1.12 mm inner diameter; World Precision Instruments) using a P-1000 puller (Sutter Instruments). Only cells showing <20 % change in access resistance throughout the recording were included; junction potentials were corrected via pipette offset. Neurons were considered responsive if their firing frequency changed by >20% during drug application.

[Protocol 1] The following compounds were tested: kisspeptin-10 (10 nM), L-NAME (1 mM), ODQ (10 μM), and DEA/NO (100 μM). Recordings were performed at 32.8 °C. The pipette solution contained (in mM): K-gluconate 140, KCl 10, EGTA 1, Na_2-ATP 2, and HEPES 10 (pH 7.3 with KOH; 290 mOsm). Following stable baseline activity, drugs were bath-applied or locally delivered using a Valve Control System (Warner Instruments). Whole-cell recordings were performed in current-clamp mode using a Multiclamp 700B amplifier (Molecular Devices). Signals were digitized with a Digidata 1550B interface and acquired using pClamp 11.4 software (Molecular Devices). Data were analyzed offline with Clampfit 11.4 (Molecular Devices) to determine mean firing rate and membrane potential before, during, and after drug application.

[Protocol 2] The following compounds were tested: kisspeptin-10 (10 nM), ODQ (10 μM), and sildenafil (30 μM). Recordings were performed at 37 °C using a temperature-controlled Luigs & Neumann chamber. The pipette solution contained (in mM): K-gluconate 120, KCl 10, HEPES 10, ATP 4, GTP 0.3, phosphocreatine 10, and EGTA 1 (pH 7.2–7.3; 280–290 mOsm). Following stable baseline activity, drugs were bath-applied. Whole-cell recordings were performed in current-clamp mode using a Multiclamp 700B amplifier (Molecular Devices). Signals were digitized with the PulseQ acquisition system (Luigs & Neumann) running in Igor Pro (Wavemetrics) and sampled at 50 kHz, low-pass filtered at 4 kHz. Data were analyzed in MATLAB to extract firing frequency and membrane potential under each condition.

Both male and female mice were used. Because the kisspeptin-10–induced change in firing rate did not differ between sexes (two-way repeated-measures ANOVA; Treatment × Sex interaction WT: $F_{(1,15)} = 1.35$, $p = 0.26$; KO: $F_{(1,16)} = 1.98$, $p = 0.18$), data from males and females are shown together in the summary graphs. However, statistical analyses were performed within each experimental subgroup, as some pharmacological conditions were applied in only one sex.

Statistical analyses

All analyses were performed using Prism 10 (Graphpad Software, San Diego, CA) and assessed for normality (Shapiro–Wilk test) and variance, when appropriate. Sample sizes were chosen according to standard practice in the field. Experimenters were blinded to group allocation during data collection and analysis. Details on biological replicates and sample sizes are provided in the figure legends. For normally distributed data, comparisons between two groups were made using a two-tailed unpaired *t*-test, or a paired *t*-test when appropriate. Comparisons among more than two groups were made using a one-way or two-way ANOVA, followed by Tukey's or Holm-Sidak's multiple-comparison post hoc test. Repeated-measures including missing values were analysed with a Mixed-effects model followed by Dunnett's test. For data not following a normal distribution, comparisons between two independent groups were made using the Mann–Whitney test. Comparisons among more than two groups were made using the Kruskal–Wallis test, followed by Dunn's post hoc test for multiple comparisons. All data are presented as mean ± s.e.m. Statistical significance was defined as $P < 0.05$. The significance levels shown in the figures are: ns, $P > 0.05$; $P < 0.05$ (*); $P < 0.01$ (**); $P < 0.001$ (***). Details on animal age, sex, and number of independent experiments are reported in the main text or figure legends.

Reporting summary

Further information on research design is available in the Nature Portfolio Reporting Summary linked to this article.

Data availability

All data supporting the findings of this study and its Supplementary Information are available from the corresponding author upon request without restrictions. Source data are provided with this paper.

References

1. Herbison, A. E. Physiology of the Adult Gonadotropin-Releasing Hormone Neuronal Network. In *Knobil and Neill's Physiology of Reproduction* (eds. Plant, T. M. & Zeleznik, A. J. B. (Fourth E.) 399–467 (Academic Press, San Diego, 2015).
2. Moenter, S. M. GnRH Neurons on LSD: A Year of Rejecting Hypotheses That May Have Made Karl Popper Proud. *Endocrinology* **159**, 199–205 (2017).
3. Clarkson, J. & Herbison, A. E. Oestrogen, kisspeptin, GPR54 and the pre-ovulatory luteinising hormone surge. *J. Neuroendocrinol.* **21**, 305–311 (2009).
4. de Roux, N. et al. Hypogonadotropic hypogonadism due to loss of function of the KiSS1-derived peptide receptor GPR54. *Proc. Natl. Acad. Sci.* **100**, 10972–10976 (2003).
5. Seminara, S. B. et al. The GPR54 gene as a regulator of puberty. *N. Engl. J. Med.* **349**, 1614–1627 (2003).
6. Funes, S. et al. The KiSS-1 receptor GPR54 is essential for the development of the murine reproductive system. *Biochem Biophys. Res Commun.* **312**, 1357–1363 (2003).
7. Oakley, A. E., Clifton, D. K. & Steiner, R. A. Kisspeptin signaling in the brain. *Endocr. Rev.* **30**, 713–743 (2009).
8. Starrett, J. R. & Moenter, S. M. Hypothalamic kisspeptin neurons as potential mediators of estradiol negative and positive feedback. *Pept. (N. Y.)* **163**, 170963 (2023).
9. Velasco, I. et al. Dissecting the KNDy hypothesis: KNDy neuron-derived kisspeptins are dispensable for puberty but essential for preserved female fertility and gonadotropin pulsatility. *Metabolism* **144**, 155556 (2023).
10. Mostari, M. stP. et al. Dynorphin-kappa opioid receptor signaling partly mediates estrogen negative feedback effect on lh pulses in female rats. *J. Reprod. Dev.* **59**, 266–272 (2013).
11. Hrabovszky, E. et al. Low degree of overlap between kisspeptin, neurokinin b, and dynorphin immunoreactivities in the infundibular nucleus of young male human subjects challenges the kndy neuron concept. *Endocrinology* **153**, 4978–4989 (2012).
12. Delli, V., Silva, M. S. B., Prévot, V. & Chachlaki, K. The KiNG of reproduction: Kisspeptin/ nNOS interactions shaping hypothalamic GnRH release. *Mol. Cell Endocrinol.* **532**, 111302 (2021).
13. Chachlaki, K. et al. Phenotyping of nNOS neurons in the postnatal and adult female mouse hypothalamus. *J. Comp. Neurol.* **525**, 3177–3189 (2017).
14. Chachlaki, K., Garthwaite, J. & Prevot, V. The gentle art of saying NO: how nitric oxide gets things done in the hypothalamus. *Nat. Rev. Endocrinol.* **13**, 521–535 (2017).
15. Chachlaki, K. & Prevot, V. Nitric oxide signalling in the brain and its control of bodily functions. *Br. J. Pharm.* **177**, 5437–5458 (2020).
16. Chachlaki, K. et al. NOS1 mutations cause hypogonadotropic hypogonadism with sensory and cognitive deficits that can be reversed in infantile mice. *Sci. Transl. Med* **14**, eabh2369 (2022).
17. Hanchate, N. K. et al. Kisspeptin-GPR54 signaling in mouse no-synthesizing neurons participates in the hypothalamic control of ovulation. *J. Neurosci.* **32**, 932–945 (2012).
18. Gyurko, R., Leupen, S. & Huang, P. L. Deletion of exon 6 of the neuronal nitric oxide synthase gene in mice results in hypogonadism and infertility. *Endocrinology* **143**, 2767–2774 (2002).
19. Rettori, V. et al. Role of nitric oxide in the control of luteinizing hormone-releasing hormone release in vivo and in vitro. *Proc. Natl. Acad. Sci. USA* **90**, 10130–10134 (1993).
20. d'Anglemont de Tassigny, X., Campagne, C., Steculorum, S. & Prevot, V. Estradiol induces physical association of neuronal nitric oxide synthase with NMDA receptor and promotes nitric oxide formation via estrogen receptor activation in primary neuronal cultures. *J. Neurochem* **109**, 214–224 (2009).
21. d'Anglemont de Tassigny, X. et al. Coupling of neuronal nitric oxide synthase to NMDA receptors via postsynaptic density-95 depends on estrogen and contributes to the central control of adult female reproduction. *J. Neurosci.* **27**, 6103–6114 (2007).
22. Parkash, J. et al. Phosphorylation of N -methyl- d -aspartic acid receptor-associated neuronal nitric oxide synthase depends on estrogens and modulates hypothalamic nitric oxide production during the ovarian cycle. *Endocrinology* **151**, 2723–2735 (2010).
23. Constantin, S., Reynolds, D., Oh, A., Pizano, K. & Wray, S. Nitric oxide resets kisspeptin-excited GnRH neurons via PIP2 replenishment. *Proc. Natl. Acad. Sci. USA* **118**, e2012339118 (2021).
24. Rameau, G. A. et al. Biphasic coupling of neuronal nitric oxide synthase phosphorylation to the nmda receptor regulates ampa receptor trafficking and neuronal cell death. *J. Neurosci.* **27**, 3445–3455 (2007).
25. Bhargava, Y. et al. Improved genetically-encoded, FlincG-type fluorescent biosensors for neural cGMP imaging. *Front Mol. Neurosci.* **6**, 26 (2013).
26. Bellefontaine, N. et al. Leptin-dependent neuronal NO signaling in the preoptic hypothalamus facilitates reproduction. *J. Clin. Invest* **124**, 2550–2559 (2014).
27. Clasadonte, J., Poulain, P., Beauvillain, J. C. & Prevot, V. Activation of neuronal nitric oxide release inhibits spontaneous firing in adult gonadotropin-releasing hormone neurons: A possible local synchronizing signal. *Endocrinology* **149**, 587–596 (2008).
28. Delli, V. et al. Male minipuberty involves the gonad-independent activation of preoptic nNOS neurons. *Free Radic. Biol. Med* **194**, 199–208 (2023).
29. Silva, M. S. B. et al. Female sexual behavior is disrupted in a pre-clinical mouse model of PCOS via an attenuated hypothalamic nitric oxide pathway. *Proc. Natl. Acad. Sci.* **119**, e2203503119 (2022).
30. Topaloglu, A. K. et al. Inactivating KISS1 Mutation and Hypogonadotropic Hypogonadism. *N. Engl. J. Med.* **366**, 629–635 (2012).
31. Herbison, A. E., d'Anglemont de Tassigny, X., Doran, J. & Colledge, W. H. Distribution and Postnatal Development of Gpr54 Gene Expression in Mouse Brain and Gonadotropin-Releasing Hormone Neurons. *Endocrinology* **151**, 312–321 (2010).
32. León, S. et al. Direct actions of kisspeptins on gnrh neurons permit attainment of fertility but are insufficient to fully preserve gonadotropic axis activity. *Sci. Rep.* **6**, 19206 (2016).
33. Wang, L. et al. Genetic dissection of the different roles of hypothalamic kisspeptin neurons in regulating female reproduction. *Elife* **8**, e43999 (2019).
34. Clarkson, J. et al. CRISPR-Cas9 knockdown of ESR1 in preoptic GABA-kisspeptin neurons suppresses the preovulatory surge and estrous cycles in female mice. *Elife* **12**, RP90959 (2023).
35. Bonavera, J. J., Sahu, A., Kalra, P. S. & Kalra, S. P. Evidence that nitric oxide may mediate the ovarian steroid-induced luteinizing hormone surge: involvement of excitatory amino acids. *Endocrinology* **133**, 2481–2487 (1993).
36. d'Anglemont de Tassigny, X., Ackroyd, K. J., Chatzidaki, E. E. & Colledge, W. H. Kisspeptin Signaling Is Required for Peripheral But Not Central Stimulation of Gonadotropin-Releasing Hormone Neurons by NMDA. *J. Neurosci.* **30**, 8581–8590 (2010).
37. Huang, P. L., Dawson, T. M., Bredt, D. S., Snyder, S. H. & Fishman, M. C. Targeted disruption of the neuronal nitric oxide synthase gene. *Cell* **75**, 1273–1286 (1993).
38. Helena, C. V. et al. KNDy neurons modulate the magnitude of the steroid-induced luteinizing hormone surges in ovariectomized rats. *Endocrinology* **156**, 4200–4213 (2015).

39. Yeo, S.-H. & Herbison, A. E. Projections of arcuate nucleus and rostral periventricular kisspeptin neurons in the adult female mouse brain. *Endocrinology* **152**, 2387–2399 (2011).
40. Caron, E., Ciofi, P., Prevot, V. & Bouret, S. G. Alteration in neonatal nutrition causes perturbations in hypothalamic neural circuits controlling reproductive function. *J. Neurosci.* **32**, 11486–11494 (2012).
41. Bouret, S. G., Draper, S. J. & Simerly, R. B. Formation of projection pathways from the arcuate nucleus of the hypothalamus to hypothalamic regions implicated in the neural control of feeding behavior in mice. *J. Neurosci.* **24**, 2797–2805 (2004).
42. Qiu, J. et al. Glutamatergic input from arcuate nucleus kiss1 neurons to preoptic kiss1 neurons is required for lh surge in female mice. *Endocrinology* **166**, bqaf015 (2025).
43. Tovar, S. et al. Effects of single or repeated intravenous administration of kisspeptin upon dynamic lh secretion in conscious male rats. *Endocrinology* **147**, 2696–2704 (2006).
44. Bentefour, Y. & Bakker, J. Kisspeptin signaling and nNOS neurons in the VMHvl modulate lordosis behavior but not mate preference in female mice. *Neuropharmacology* **198**, 108762 (2021).
45. Kreisman, M. J., McCosh, R. B. & Breen, K. M. A Modified Ultra-Sensitive ELISA for Measurement of LH in Mice. *Endocrinology* **163**, bqac109 (2022).
46. Lein, E. S. et al. Genome-wide atlas of gene expression in the adult mouse brain. *Nature* **445**, 168–176 (2007).
47. Batchelor, A. M. et al. Exquisite sensitivity to subsecond, picomolar nitric oxide transients conferred on cells by guanylyl cyclase-coupled receptors. *Proc. Natl. Acad. Sci. USA* **107**, 22060–22065 (2010).

Acknowledgements

This work has been supported by the ANR JCJC No ANR-25-CE16-4904 INFERNO and Fondation Université Lille FUL-GENIE (to K.C.), the European Union Horizon 2020 research and innovation program No 847941 miniNO (to A.C.), the Société Française d'étude de la Fertilité (SFEF) (MSc fellowship to J.D.), and the University of Lille (PhD fellowship to V.D.). The authors would like to acknowledge Dr Vincent Prevot for the grants European Research Council (ERC) Synergy grant No 810331 WATCH, the DistAlz (ANR-11-LABEX-0009), European Genomic Institute for Diabetes (EGID, ANR-10-LABX-0046) and the I-SITE ULNE (ANR-16-IDEX-0004) that enabled part of this research. The authors thank Prof John Garthwaite and Dr Vincent Prevot for intellectual discussions; Dr Mauro S.B. Silva and Dr Paolo Giacobini for their advice in designing the viral strategies used; Dr Meryem Tardivel-Safi and Antonino Bongiovanni (imaging core facility, BiCeL) and Julien Devassine (animal house) of the UMS2014-US41 for their expert technical assistance. Graphics were created in BioRender.Chachlaki, K. (2026) https://BioRender.com/arnv9ca. This work is dedicated to the memory of Prof John Garthwaite, a pioneer of nitric oxide research and an extraordinary mentor, wise, generous and kind, deeply loved and admired by all who had the privilege of knowing him. He created and characterized the FlincG3 biosensor used in this study, which enabled our investigations of cGMP signaling in neurons. He will be deeply missed, yet his unwavering enthusiasm for science will continue to inspire us.

Author contributions

K.C. and V.D. conceived and designed the study. V.D., M.M., D.L., A.C., and K.C. prepared the figures. V.D., A.-M.L., C.-A.S., J.D., D.F., and K.C. performed and analyzed mouse studies. T.L., M.M., D.L. and A.C. performed and analyzed electrophysiological recordings. S.N. and K.C. performed and analyzed FlincG3 experiments. K.C. drafted the manuscript. V.D., D.L., M.M., and A.C. contributed to writing specific sections and to figure preparation. S.R. provided substantive editorial input and assisted in shaping the final version. All authors reviewed and approved the final manuscript.

Competing interests

The authors declare no competing interests.

Additional information

Supplementary information The online version contains supplementary material available at https://doi.org/10.1038/s41467-026-69316-0.

Correspondence and requests for materials should be addressed to Konstantina Chachlaki.

Peer review information *Nature Communications* thanks Waljit Dhillo, Chayarndorn Phumsatitpong, and Joern Steinert for their contribution to the peer review of this work. A peer review file is available.